

**Détection de rayonnements
à très basse température**

5e école thématique du 2 au 8 juin 2002

ON-CHIP MICROCOOLING

J.PEKOLA

**Department of Physics
University of Jyväskylä
FINLAND**

Oléron

Efficient electronic cooling in heavily doped silicon by quasiparticle tunneling

A. M. Savin

Department of Physics, University of Jyväskylä, P.O. Box 35, FIN-40351 Jyväskylä, Finland

M. Prunnila^{a)}

VTT Electronics, P.O. Box 1101, FIN-02044 VTT, Finland

P. P. Kivinen and J. P. Pekola

Department of Physics, University of Jyväskylä, P.O. Box 35, FIN-40351 Jyväskylä, Finland

J. Ahopelto

VTT Electronics, P.O. Box 1101, FIN-02044 VTT, Finland

A. J. Manninen

Nokia Research Center, P.O. Box 407, FIN-00045 Nokia Group, Jyväskylä, Finland

(Received 18 May 2001; accepted for publication 3 July 2001)

Cooling of electrons in a heavily doped silicon by quasiparticle tunneling using a superconductor–semiconductor–superconductor double-Schottky-junction structure is demonstrated at low temperatures. In this work, we use Al as the superconductor and thin silicon-on-insulator (SOI) film as the semiconductor. The electron–phonon coupling is measured for the SOI film and the low value of the coupling is shown to be the origin of the observed significant cooling effect. © 2001 American Institute of Physics. [DOI: 10.1063/1.1399313]

Success in development of low-temperature microcoolers based on normal metal–insulator–superconductor (NIS) junctions stimulates intensive attempts to improve their performance and to make them suitable for technical applications.^{1–6} Cooling of the electron system in a normal metal^{1,2,4} and quasiparticles in a superconductor,³ and also cooling of the lattice of a thermally isolated system,⁶ have been demonstrated using NIS junctions. One unexplored approach is to use a heavily doped semiconductor instead of a normal metal in the cooler device. In this approach, the superconductor can be brought into metallurgical contact with the semiconductor and the Schottky barrier in the semiconductor–superconductor (Sm–S) contact will form the tunnel barrier. From practical and technological points of view, heavily doped silicon would be the best choice as the semiconductor. Especially, the use of silicon-on-insulator (SOI) substrates as a starting material would make the utilization of standard silicon micromachining techniques relatively easy in the fabrication of thermally isolated self-standing structures, which are required for lattice refrigeration.

At low temperatures the electron–phonon (EP) coupling is weak, which leads to a large relative temperature difference between the phonons and electrons even when a relatively small heat flow is introduced through the EP system. The strength of the EP coupling is one of the key issues in the performance of a low-temperature cooler. In this letter, we show that the (very) weak EP coupling in heavily doped silicon leads to efficient cooler performance in an Al– n^+ –SOI–Al superconductor–semiconductor–superconductor (S–Sm–S) structure.

^{a)}Electronic mail: mika.prunnila@vtt.fi

Operation of a S–Sm–S cooler is depicted in Fig. 1. The cooling of the normal electrode (semiconductor) can be observed at low temperatures when $k_B T \ll \Delta$ (Δ is the superconducting energy gap) if a small voltage $V < 2\Delta/e$ is applied across the structure. At small bias only the most energetic electrons in the thermal tail of the Fermi distribution can tunnel from the semiconductor through the left Schottky junction to the superconductor. On the other hand, the quasiparticles below the energy gap in the right superconductor can tunnel to the semiconductor. The net effect is now that electrons are removed above (Sm→S tunneling in Fig. 1) and added below the Fermi level (S→Sm tunneling in Fig. 1) in the semiconductor. This reduces the total energy of the electron gas and leads to the cooling effect. For a weak cou-

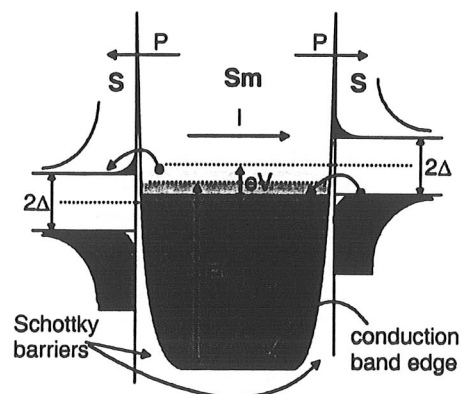


FIG. 1. Energy-band diagram illustrating cooling in the S–Sm–S structure. S denotes superconductor and Sm semiconductor. 2Δ is the energy gap in the superconductor, E_f the Fermi energy of the semiconductor, and P heat flow out of the semiconductor. V is the applied voltage and I is the resulting current. The gray areas denote occupied (single-particle) electron states.

pling BCS superconductor, the maximum cooling power for a S–Sm–S cooler with two symmetric junctions is given by^{2,6}

$$P_{\max} \approx 2 \times 0.6 \frac{\sqrt{\Delta}}{e^2 R_T} (k_B T_e)^{3/2}, \quad (1)$$

where R_T is the tunneling resistance for a single junction and T_e is the electron temperature in the semiconductor. The maximum cooling power is obtained when the voltage drop across a single junction is slightly below Δ/e .

At low temperatures there are no thermally excited optical phonons and the energy transfer between the electrons and crystal lattice is mediated by the electron–acoustic-phonon interaction. In this case, the EP heat flow is given by^{7,8}

$$P_{\text{el-ph}} = \Sigma \Omega (T_e^5 - T_0^5), \quad (2)$$

where $T_e(T_0)$ is the temperature of electrons (phonons), Ω is the volume of the system, and Σ is a material-dependent constant. We have chosen the heat flow from electrons to phonons to be the positive direction. Here, the experimental studies are performed using a thin degenerate SOI film, and it is assumed that the temperature of the phonon system is equal to the temperature of the substrate. This assumption requires that the thermal resistance between the sample film and the substrate is small compared to the thermal resistance between the electron and the phonon systems in the film. When heat flow originates from the S–Sm–S cooling effect, we can write $P_{\max} + P_{\text{el-ph}} = 0$. The coupling constant Σ in Eq. (2) can be estimated independently by Joule heating the electron system.

The samples were fabricated on a bonded SOI wafer with a 100-nm-thick SOI film and 400-nm-thick buried-oxide (BOX) layer. The mesas were etched in Cl_2/He plasma using an UV-patterned photoresist as an etching mask. The wafers were then implanted with phosphorous to a dose of $5 \times 10^{14} \text{ cm}^{-2}$ at 20 keV, followed by oxidation in dry ambient at 1000 °C. Contact windows were then opened in buffered hydrofluoric (BHF) acid, and after a HF dip a 300-nm-thick aluminum layer was deposited by sputtering. The aluminum film was sintered at 400 °C. We used Al–1% Si in order to prevent silicon dissolution in the contacts (junction spiking) during the sintering step. The final thickness of the SOI film was measured to be $4 \times 10^{19} \text{ cm}^{-3}$, which is enough to make silicon a “metallic” conductor.⁹ A $^3\text{He}/^4\text{He}$ dilution refrigerator was used in the measurements and it was assumed that the phonon temperature of the substrate was the same as that of the copper sample holder. Quasiparticle tunneling is very sensitive to the electron temperature of the normal electrode, but virtually insensitive to the temperature of the superconductor, and it can be used as a temperature probe with negligible heat leaks.^{1,2,10} We used extra pairs of current biased Sm–S junctions to probe the electronic temperature in the SOI film. These S–Sm–S thermometers were calibrated against the thermometer of the copper sample holder.

The current–voltage characteristics of a S–Sm–S test structure in the temperature range of 0.16–1.34 K are shown in Fig. 2. The characteristics clearly exhibit the well-known

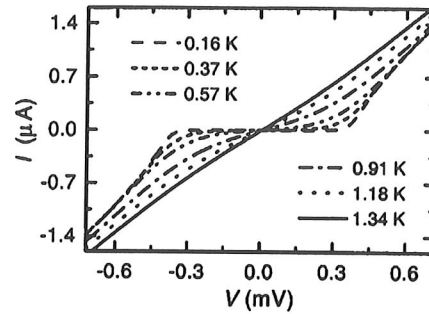


FIG. 2. Current–voltage characteristics of a S–Sm–S test structure with $10 \times 30 \mu\text{m}^2$ Schottky junctions.

features of (double) NIS tunneling.¹¹ Figure 3(a) shows an optical micrograph of a $20 \times 30 \mu\text{m}^2$ S–Sm–S cooler and schematic coupling to the measurement circuitry. The schematic cross section is depicted in Fig. 3(b). The device had $5 \times 18 \mu\text{m}^2$ cooling junctions and $3 \times 3 \mu\text{m}^2$ thermometer junctions. The tunneling resistance of the cooler contacts was estimated to be 800Ω . This value was obtained from the normal-state resistance of the contacts measured at 4.2 K. The electron temperature in the n^{++} SOI film as a function of the voltage across the S–Sm–S cooler at different substrate temperatures is shown in Fig. 3(c). Two clear minima can be seen in the temperature dependence at $V \approx \pm 0.34 \text{ mV}$ for all the curves. These values are slightly below twice the gap of aluminum, $2\Delta/e \approx 400 \mu\text{V}$, as expected. Even though the

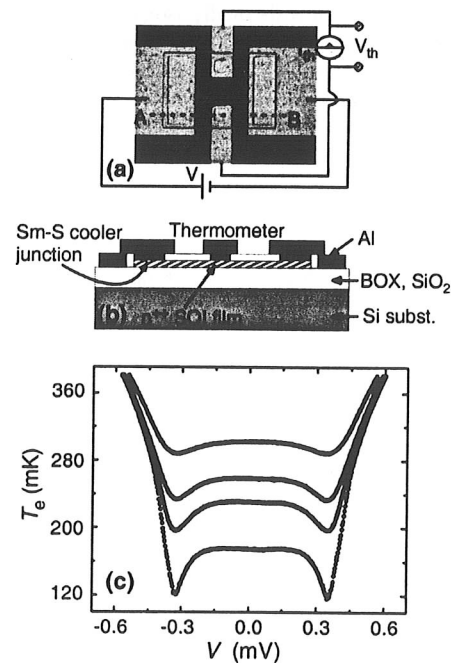


FIG. 3. (a) Optical micrograph of a S–Sm–S cooler device and schematic illustration of the connections to external circuitry in the measurements. Current I_{th} and voltage V_{th} are used in determining the electronic temperature T_e in the n^{++} SOI mesa. (b) Schematic cross section of the device along the line AB in (a). (c) The electron temperature in n^{++} SOI as a function of the voltage across the S–Sm–S cooler structure at different substrate temperature T_0 .

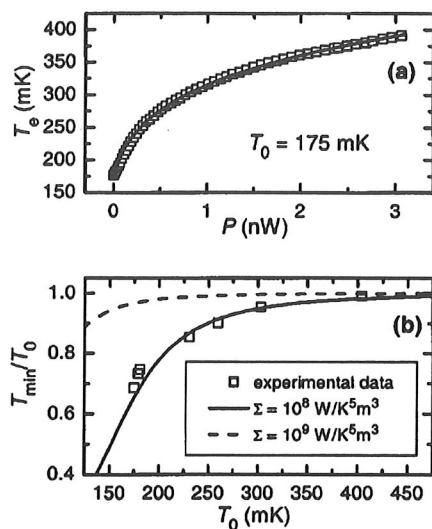


FIG. 4. (a) Electron temperature as a function of heating power for a large $100 \times 750 \mu\text{m}^2$ sample at $T_0 = 175 \text{ mK}$. The solid line is the result of the fitting of experimental data with Eq. (2). (b) Relative minimum electron temperature T_{min}/T_0 as a function of phonon temperature T_0 . Experimental points are measured from the sample in Fig. 3(a). Solid (dashed) curve corresponds to numerical solution of $P_{\text{max}} + P_{\text{el-ph}} = 0$ with $\Sigma = 1.0 \times 10^8 \text{ W/K}^5 \text{ m}^3$ ($\Sigma = 1.0 \times 10^9 \text{ W/K}^5 \text{ m}^3$).

volume of the device and the tunneling resistances of the junctions are rather large, we observe significant cooling of the electron system: it exceeds 30% at $T_0 = 175 \text{ mK}$. By determining the strength of the EP coupling independently, we will show that the magnitude of the cooling is mediated by the very small EP coupling.

We used a rectangular sample of area of $100 \times 750 \mu\text{m}^2$ to deduce the coupling constant Σ in Eq. (2). The biasing scheme in this experiment was similar to that of the cooling experiment. However, a sufficiently large current was applied along the long axis of the sample to heat up the electrons. Another small current was applied at the center across the sample for temperature measurement. The electron temperature as a function of the heating power is presented in Fig. 4(a). The fit of Eq. (2) to the experimental data with $\Sigma = 1.0 \times 10^8 \text{ W/K}^5 \text{ m}^3$ is nearly perfect. This value is about one order of magnitude smaller than the EP coupling constant in normal metals^{12,13} and it is few times smaller than the EP coupling constant in aluminum.^{14,15} Fitting the experimental data using Eq. (2) with the exponent as a parameter gives us a value of the exponent in the range of 4.8–5.3.

Figure 4(b) shows the experimental and calculated relative minimum electron temperature of the cooler structure as a function of the phonon temperature. The experimental points are obtained from the minima of $T_e - V$ curves [four such curves are shown in Fig. 3(c)] measured from the S–Sm–S cooler in Fig. 3(a). The minimum temperature corresponds to the maximum cooling power. The solid line in Fig. 4(b) is a numerical solution of the electronic temperature from the equation $P_{\text{max}} + P_{\text{el-ph}} = 0$ with $\Sigma = 1.0 \times 10^8 \text{ W/K}^5 \text{ m}^3$, $\Delta = 200 \mu\text{eV}$, $\Omega = 20 \times 30 \times 70$

$\times 10^{-3} \mu\text{m}^3$, and $R_T = 800 \Omega$. The line fits well to the experimental data. For comparison, we have also shown a solution with $\Sigma = 1.0 \times 10^9 \text{ W/K}^5 \text{ m}^3$ corresponding to a typical normal metal sample. With this higher value for the coupling constant Σ , the cooling effect is small. Therefore, an Al–n⁺⁺–Si–AlS–Sm–S cooler can attain lower electron temperature when compared to a similar metal-based SINIS cooler due to the lower EP coupling. However, the cooling power of our device is rather low, e.g., at $T_0 = 175 \text{ mK}$ $P_{\text{max}} \approx 0.5 \text{ pW}$. The low power arises from the high tunneling resistances. For our samples the contact resistivity of the Al–Si junctions is $\sim 7 \times 10^{-4} \Omega \text{ cm}^2$. By increasing the doping level to $\sim 10^{20} \text{ cm}^{-3}$ the contact resistivity should decrease by a few orders of magnitude.¹⁶ This would increase the cooling power to a range that is adequate for device applications.¹⁷

In summary, we have demonstrated significant cooling of electrons in heavily doped silicon film by quasiparticle tunneling through semiconductor–superconductor Schottky junctions at sub-Kelvin temperatures. The relatively strong cooling effect was shown to arise from a weak electron–phonon coupling in heavily doped silicon. The EP coupling was estimated using a Joule heating experiment. The weak EP coupling and the demonstrated cooling effect make heavily doped silicon films very promising candidates for low-temperature on-chip cooling applications.

The authors gratefully acknowledge M. Markkanen's contribution in sample fabrication. This work has been partly funded by the Academy of Finland. One of the authors (M.P.) acknowledges financial support also from the Graduate School in Electronics, Telecommunications and Automation (GETA).

- ¹M. Nahum, T. M. Eiles, and J. M. Martinis, Appl. Phys. Lett. **65**, 3123 (1994).
- ²M. M. Leivo, J. P. Pekola, and D. V. Averin, Appl. Phys. Lett. **68**, 1996 (1996).
- ³A. J. Manninen, J. K. Suoknuuti, M. M. Leivo, and J. P. Pekola, Appl. Phys. Lett. **74**, 3020 (1999).
- ⁴R. Leoni, G. Arena, M. G. Castellano, and G. Torrioli, J. Appl. Phys. **85**, 3877 (1999).
- ⁵J. P. Pekola, D. V. Anghel, T. I. Suppala, J. K. Suoknuuti, A. J. Manninen, and M. Manninen, Appl. Phys. Lett. **76**, 2782 (2000).
- ⁶A. Luukanen, M. M. Leivo, J. K. Suoknuuti, A. J. Manninen, and J. P. Pekola, J. Low Temp. Phys. **120**, 281 (2000).
- ⁷P. B. Allen, Phys. Rev. Lett. **59**, 1460 (1987).
- ⁸F. C. Wellstood, C. Urbina, and John Clarke, Phys. Rev. B **49**, 5942 (1994).
- ⁹M. N. Alexander and D. F. Holcomb, Rev. Mod. Phys. **40**, 815 (1968).
- ¹⁰M. Nahum and J. M. Martinis, Appl. Phys. Lett. **63**, 3075 (1993).
- ¹¹See, e.g., M. Tinkham, *Introduction to Superconductivity*, 2nd ed. (McGraw-Hill, New York, 1996).
- ¹²Y. Shinba, K. Nakamura, M. Fukuchi, and M. Sakata, J. Phys. Soc. Jpn. **51**, 157 (1982).
- ¹³M. L. Roukes, M. R. Freeman, R. S. Germain, and R. C. Richardson, Phys. Rev. Lett. **55**, 422 (1985).
- ¹⁴R. L. Kautz, G. Zimmerli, and J. M. Martinis, J. Appl. Phys. **73**, 2386 (1993).
- ¹⁵J. P. Kauppinen and J. P. Pekola, Phys. Rev. B **54**, 8353 (1996).
- ¹⁶C. Y. Chang, Y. K. Fang, and S. M. Sze, Solid-State Electron. **14**, 541 (1971).
- ¹⁷D. V. Anghel, A. Luukanen, and J. P. Pekola, Appl. Phys. Lett. **78**, 556 (2001).

Refrigeration of a dielectric membrane by superconductor/insulator/normal-metal/insulator/superconductor tunneling

A. J. Manninen,^{a)} M. M. Leivo, and J. P. Pekola
Department of Physics, University of Jyväskylä, FIN-40351 Jyväskylä, Finland

(Received 2 December 1996; accepted for publication 5 February 1997)

We have applied tunneling of electrons between a normal metal and a superconductor to refrigerate a thin dielectric membrane attached to the normal electrode of a superconductor/insulator/normal-metal/insulator/superconductor (SINIS) structure. Starting from $T \approx 200$ mK, a decrease in temperature of several mK was observed, measured by a separate thermometer on the membrane. It should be straightforward to improve the refrigerator performance to the level of the recently demonstrated SINIS electron cooling method, such that the drop in the lattice temperature would be more than an order of magnitude larger. © 1997 American Institute of Physics. [S0003-6951(97)04914-0]

When electrons tunnel through an insulating barrier between a normal metal and a superconductor, the electronic temperature of the normal metal can decrease.¹⁻³ This phenomenon, *cooling* of electrons by normal-metal/insulator/superconductor (NIS) tunneling, has recently been observed experimentally.^{1,2} In these experiments, only the electrons of the normal metal cool but the phonons remain at bath temperature. This can happen because of thermal decoupling of the electrons from the lattice at low temperatures. In this letter we show that it is possible to use the NIS junctions to *refrigerate* the lattice and other samples, as well, if the normal electrode is thermally isolated from the surroundings by fabricating it on a thin dielectric membrane.

The cooling effect in NIS junctions is based on the existence of the energy gap Δ in the superconductor. $N \rightarrow S$ tunneling through a junction with bias voltage V is not possible for electrons with energy E between $E_F - eV - \Delta$ and $E_F - eV + \Delta$, because there are no states in the superconductor in that energy interval. Thus, when $V < \Delta/e$, only electrons with E exceeding the Fermi energy E_F can tunnel from the normal metal to the superconductor at temperatures well below the transition temperature T_c (such that the energy states below the gap in the superconductor are full).¹ With opposite polarity, the electrons that tunnel from the superconductor to the normal metal have $E < E_F$. In both cases, the step at E_F in the distribution function of the electrons in the normal metal becomes sharper, i.e., the system cools down. Cooling power \dot{Q} can be calculated in the same way as the tunneling electric current,⁴ but now we must consider that each electron carries energy ε . Setting the zero of the energy to the Fermi level of the normal metal, we get

$$\dot{Q}(V) = \frac{1}{e^2 R_T} \int_{-\infty}^{+\infty} [f(\varepsilon, T_{e,n}) - f(\varepsilon - eV, T_{e,s})] \times N(\varepsilon - eV) \varepsilon d\varepsilon, \quad (1)$$

where $N(\varepsilon) = \Theta(\varepsilon^2 - \Delta^2) |\varepsilon| / \sqrt{\varepsilon^2 - \Delta^2}$ is the density of states in the superconductor, R_T is the normal-state tunneling resistance of the junction, $f(\varepsilon, T)$ is the Fermi distribution function, and $T_{e,n}$ and $T_{e,s}$ are the electronic temperatures of

the normal and the superconducting electrode, respectively. When $T \ll T_c$, maximum cooling power is achieved when $|V|$ is only slightly below Δ/e , and it is

$$\dot{Q}_{\max} = \alpha(T_{e,n}) \frac{\Delta^2}{e^2 R_T} \left(\frac{k_B T_{e,n}}{\Delta} \right)^{3/2}, \quad (2)$$

where $\alpha(T_{e,n}) \approx 0.6$. This method has been used to cool electrons in a normal metal from 300 to 100 mK in a superconductor/insulator/normal-metal/insulator/superconductor (SINIS) structure, which consists of a normal island between two superconducting electrodes.² In that structure, the electric current flows into the normal island through one junction and out through the other, but heat flows away from the normal island through both junctions.

NIS tunneling cools directly the electrons of the normal metal. The phonon system can be refrigerated via the electron-phonon coupling: heat flow from phonons (temperature T_p) to electrons (temperature T_e) is given as

$$\dot{Q}_{e-p} = \Sigma U (T_p^5 - T_e^5), \quad (3)$$

where U is the volume of the normal electrode, and Σ is a material-dependent constant of order 10^9 W/K⁵ m³ (see, however, Ref. 5). At low temperatures the electron-phonon coupling is very small and can be the bottleneck of heat transfer from the surroundings to the electrons of the normal island. This was the case in the earlier experiments^{1,2} in which the samples were made of thin copper (normal) and aluminum (superconducting) films evaporated directly on a thick silicon substrate. Only the electrons in copper cooled down, while the lattice remained presumably very near to the temperature of the substrate, which was thermally anchored to the dilution refrigerator. In order to refrigerate the lattice noticeably, there must be a thermal resistance between the normal electrode and the substrate, which is not too small compared to that between electrons and phonons. We have achieved this by extending the normal electrode on a thin dielectric membrane. Earlier, Nahum and co-workers^{1,6} have suggested a refrigerator based on a single NIS junction fabricated on a dielectric membrane.

The schematic layout of our refrigerator is shown in Fig. 1. Substrate material is silicon with a thin Si₃N₄ film on the surface. In the middle of the chip there is a 700×700 μm² window made of a 0.2 μm thick silicon nitride mem-

^{a)}Electronic mail: a_manninen@jyfl.jyu.fi

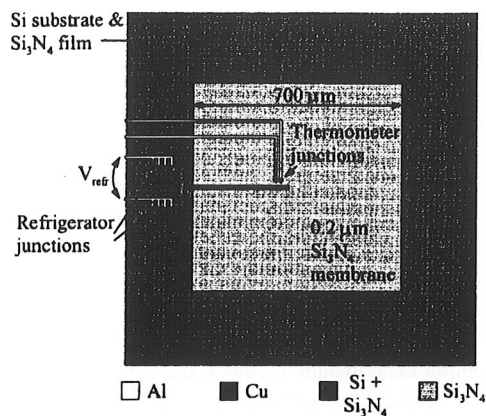


FIG. 1. Schematic layout of the SINIS refrigerator fabricated partly on a silicon nitride membrane. For clarity, the shadow images formed in the two-angle evaporation process have been omitted. Note that most of the vertical lines actually consist of a copper film on top of an oxidized aluminum film.

brane, formed by etching silicon away. The refrigerator is of SINIS type, superconducting parts made of a 30 nm thick aluminum film, the normal island made of a 35 nm thick copper film, and the tunnel junctions formed by oxidized aluminum. Electron beam lithography and two-angle evaporation techniques were used. The refrigerator junctions were fabricated on a bulk substrate, i.e., outside the thin membrane, in good thermal contact with the dilution refrigerator. Several junctions were made in parallel as a comblike structure, to enhance the cooling power. The copper island was extended onto the silicon nitride membrane, whose temperature was determined with another SINIS structure using the same method as in Ref. 7; the voltage across the two junctions was measured at constant bias current that was set to be small enough not to contribute to heat transport (see also Ref. 2). The thermometer was calibrated against the primary Coulomb blockade thermometer.⁸

Data are presented for two samples, sample 1 and sample 2. Both "refrigerator combs" of sample 1 consisted of 20 parallel $0.3 \times 0.3 \mu\text{m}^2$ junctions. The tunneling resistance across the combs was $130 \Omega + 130 \Omega$. The size of the extension of the copper island on the membrane was $280 \mu\text{m} \times 1 \mu\text{m} \times 35 \text{ nm}$ (see Fig. 1). The tunnel junctions of the thermometer were located on the membrane about $2 \mu\text{m}$ away from the extension of the refrigerator, and their total resistance was $8.4 \text{ k}\Omega$. There was no electrical contact between the refrigerator and the thermometer. The refrigerator combs of sample 2 were made of ten $0.3 \times 1 \mu\text{m}^2$ junctions, and the tunneling resistance across the combs was about $350 \Omega + 350 \Omega$. The extension of the copper island in sample 2 had a T-shape, with a $1.5 \times 250 \mu\text{m}^2$ line on the membrane connected to the substrate with a perpendicular $0.5 \times 160 \mu\text{m}^2$ line.

Refrigeration traces of sample 1 at several temperatures are plotted in Fig. 2. The silicon substrate remains at the temperature T_0 of the dilution refrigerator, while the temperature T_m of the membrane can be decreased by applying a voltage V_{refr} across the refrigerator junctions. First the elec-

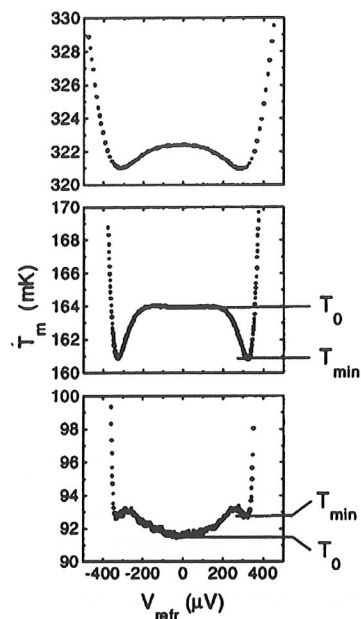


FIG. 2. Membrane temperature T_m as a function of the voltage V_{refr} across the refrigerator junctions for sample 1 at substrate temperatures $T_0 = 322, 164,$ and 92 mK .

trons near the junctions are cooled below the lattice temperature T_0 by tunneling current, then the electrons further away on the copper island are refrigerated via thermal conduction, and finally the copper lattice on the membrane, and the membrane itself, are refrigerated because of electron-phonon coupling. Refrigeration effect is strongest when $|V_{\text{refr}}| \approx 330 \mu\text{V}$, which is slightly below $2\Delta/e$ ($\approx 360 \mu\text{V}$ for this sample), as expected; factor 2 is due to the two tunnel junctions in series in the SINIS structure. As T_0 is decreased, the temperature dips become narrower, as in electronic cooling experiments.² At the very lowest temperatures, the refrigeration is overshadowed by heating caused probably by resistive current paths through pinholes in tunnel junctions. Dissipation caused by electric current flowing across the copper island with estimated resistance of about 50Ω cannot produce such heating at low voltages, because tunneling current is negligible when $V \ll 2\Delta/e$.

The traces in Fig. 2 were measured using ac techniques: the voltage across the refrigerator junctions was alternated between 0 and V_{refr} at frequency $f \approx 5 \text{ Hz}$, and the thermometer response was monitored using a lock-in amplifier with reference f . This method could be used because the thermal time constant of the system is short enough, under $10 \mu\text{s}$. The results were consistent with those of the dc measurements, but the noise level was smaller by more than an order of magnitude.

Figure 3 shows the temperature dependence of the maximum decrease in membrane temperature, $T_{\text{min}} - T_0$, for the two samples. For both samples, the refrigeration effect is largest at $T_0 \approx 200 \text{ mK}$. At higher temperatures, the refrigeration becomes weaker; the cooling power of the SINIS increases as $T^{3/2}$ [see Eq. (2)], but the heat load via the mem-

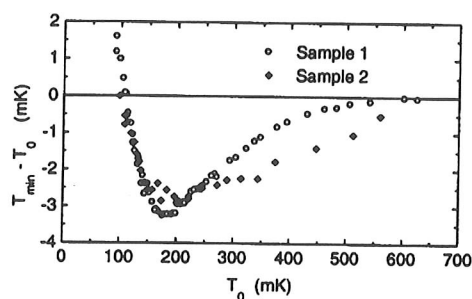


FIG. 3. Maximum decrease in membrane temperature, $T_{\min} - T_0$, as a function of the substrate temperature T_0 for two samples. See Fig. 2 for definition of T_{\min} .

brane increases even faster, because the thermal conduction along a thin silicon nitride film has a T^3 temperature dependence.⁹ Moreover, the heat flow from phonons to electrons on that part of the copper island, which was fabricated on the bulk substrate (where the phonon system of copper stays at substrate temperature), increases with temperature according to Eq. (3). The latter effect is especially important in sample 1, in which the volume of copper outside the membrane is relatively large, about 35% of the total volume of the island. The temperature of the membrane, T_m , can be higher than that of the electrons in the normal electrode near the junctions, mainly because of the thermal resistance across the copper film. Electron-phonon coupling is so strong and Kapitza resistance between copper and silicon nitride so small that T_m is very nearly equal to the electronic temperature $T_{e,m}$ of copper on the membrane; this was confirmed in one of our samples, in which both T_m and $T_{e,m}$ were measured.

The obvious explanation for the decrease of the refrigeration effect when $T_0 < 200$ mK would be thermal decoupling of phonons and electrons. At temperatures low enough, the temperature of the lattice would not decrease much even if the electrons could be cooled down to zero temperature. However, we have observed a similar deterioration in performance at low temperatures in electron cooling experiments, as well. That is partly caused by the heating effect observed in the lowest trace of Fig. 2, and by Ohmic dissipation in current transported through the resistive copper island. It is also possible that the heat brought into the superconductor by the tunneling electrons is not removed effectively enough. In order to decrease the cooling power noticeably, the temperature of the electron system in the superconductor near the tunnel junction should be about $0.3T_c \approx 400$ mK, which is not unrealistically high, although we did not measure it.

Our construction, in which the refrigerator junctions are located on the bulk substrate, ensures that heat generated by tunneling electrons is dumped away from the refrigerated membrane. However, it also means that near the junctions, the lattice of the normal electrode stays at the substrate temperature T_0 . That limits the use of the refrigerator to temperatures below about 1 K, even if one uses superconductors that have higher T_c than aluminum; if $T_0 \gg 1$ K, electron-phonon coupling is too strong to allow cooling of electrons substantially below T_0 . It remains to be tested whether the

lattice of the normal electrode near the junctions could be refrigerated below T_0 by fabricating the junctions onto the membrane,⁶ even though the heat brought into the superconductor, $\dot{Q} + IV_{\text{refr}}$, is about an order of magnitude larger than the cooling power \dot{Q} .

The performance of the refrigerator can be improved substantially at subkelvin temperatures. Our experiments have indicated that if we can cool the electrons in a normal metal film fabricated on a thin dielectric membrane, the temperature of the membrane can decrease by the same amount. Thus, nothing should prevent developing the present method to the level that has been demonstrated in earlier SINIS electron cooling experiments, in which the temperature of electrons has been decreased down to about 1/3 of the starting value.² That would already be useful in some practical applications. The most straightforward improvement would be to increase the number of refrigerator junctions. Other ways to increase the cooling power would be to decrease the resistance of individual tunnel junctions or to replace aluminum with a superconductor having larger Δ . The temperature drop of the membrane could be increased also by decreasing the thermal conduction along it. One could use a thinner membrane or make holes through it to decrease the conduction area.

To conclude, we have shown that it is possible to use NIS tunneling not only to *cool* the electrons of the normal electrode themselves but also to *refrigerate* other, electrically separate systems. The normal island of a SINIS structure was extended onto a dielectric membrane whose temperature was monitored with a separate thermometer. So far, we have demonstrated a 2% temperature decrease in the membrane, but it should be straightforward to develop the techniques to the level of reaching 100 mK from a starting temperature of 300 mK, which has been obtained in electron cooling experiments.² It will be much more difficult to reach temperatures much below 100 mK, as well as to make the refrigerator work at $T > 1$ K. However, a SINIS refrigerator will be a much simpler alternative to the dilution refrigerator in certain applications below 1 K.

The authors thank Yu. Pashkin and D. Averin for discussions and the Academy of Finland for financial support.

¹M. Nahum, T. M. Eiles, and J. M. Martinis, *Appl. Phys. Lett.* **65**, 3123 (1994).

²M. M. Leivo, J. P. Pekola, and D. V. Averin, *Appl. Phys. Lett.* **68**, 1996 (1996).

³A. Bardas and D. Averin, *Phys. Rev. B* **52**, 12 873 (1995).

⁴L. Solymar, *Superconductive Tunneling and Applications* (Chapman and Hall, London, 1972), Sec. 4.5.

⁵J. P. Kauppinen and J. P. Pekola, *Phys. Rev. B* **54**, R8353 (1996).

⁶P. A. Fisher, J. N. Ullom, and M. Nahum, *J. Low Temp. Phys.* **101**, 561 (1995).

⁷M. Nahum and J. M. Martinis, *Appl. Phys. Lett.* **63**, 3075 (1993).

⁸J. P. Pekola, K. P. Hirvi, J. P. Kauppinen, and M. A. Paalanen, *Phys. Rev. Lett.* **73**, 2903 (1994).

⁹W. Holmes and P. L. Richards (private communication).

Cooling of a superconductor by quasiparticle tunneling

A. J. Manninen,^{a)} J. K. Suoknuuti, M. M. Leivo, and J. P. Pekola
Department of Physics, University of Jyväskylä, FIN-40351 Jyväskylä, Finland

(Received 25 January 1999; accepted for publication 23 March 1999)

We have extended the cryogenic cooling method based on tunneling between a superconductor and another metal to the case when both metals are superconducting but when their energy gaps are different; earlier, this method was applied between a superconductor and a normal metal. The electron system of a titanium strip with the superconducting transition temperature $T_{c2}=0.51$ K has been cooled from $1.02T_{c2}$ to below $0.7T_{c2}$ by this method, using aluminum as the other superconductor. © 1999 American Institute of Physics. [S0003-6951(99)02320-7]

A cryogenic refrigeration method based on normal metal–insulator–superconductor (NIS) tunneling has been developed during recent years. After the first demonstration of the operation principle,¹ the electrons in a small normal metal island have been cooled from 300 down to 100 mK using this technique.² Refrigeration of a dielectric membrane has been demonstrated, too.^{3,4} In this letter, we show that the tunneling method can be applied to cool down the electrons in a superconductor, as well.

Let us consider tunneling between two different superconductors, S_1 and S_2 , with energy gaps Δ_1 and Δ_2 , respectively. We assume that $\Delta_2 < \Delta_1$. As in the NIS case,¹⁻⁴ which corresponds to $\Delta_2 = 0$, there is a heat flow

$$\dot{Q} = \frac{1}{e^2 R_T} \int_{-\infty}^{\infty} [f(\epsilon, T_{e2}) - f(\epsilon - eV, T_{e1})] \times N_2(\epsilon) N_1(\epsilon - eV) \epsilon d\epsilon \quad (1)$$

from S_2 through the S_2/S_1 junction which is biased at voltage V . Here $N_i(\epsilon) = \Theta(\epsilon^2 - \Delta_i^2) |e| / \sqrt{\epsilon^2 - \Delta_i^2}$ is the normalized BCS density of states in the superconductor S_i , R_T is the normal-state tunneling resistance of the junction, $f(\epsilon, T)$ is the Fermi distribution function, and T_{ei} is the temperature of electrons in S_i . Figure 1 shows the calculated cooling power \dot{Q} as a function of V for different values of Δ_2 at a constant temperature. When $eV < \Delta_1 + \Delta_2$, $\dot{Q} > 0$ and S_2 cools down. This is understandable, because only the ‘‘hot’’ quasiparticle excitations from above the energy gap Δ_2 can tunnel from S_2 to S_1 , which has free quasiparticle states only above the gap when $k_B T_{e1} \ll \Delta_1$. \dot{Q} is symmetric with respect to V , allowing connection of two junctions in series as in the NIS case.²

For comparison, we have also plotted the cooling power of an NIS junction in Fig. 1. The maximum is reached when $|V|$ is slightly below Δ_1/e , and it is approximately $\dot{Q}_{\max}^{\text{NIS}} \approx 0.6e^{-2} R_T^{-1} \Delta_1^{1/2} (k_B T_{e2})^{3/2}$ when $k_B T_{e1} \ll \Delta_1$.² As Fig. 1 shows, the cooling power of an S_2/S_1 junction can be even larger than that of the NIS junction, as long as Δ_2 is small enough compared to Δ_1 and temperature is not too much lower than Δ_2/k_B (such that there is a finite density of quasiparticle excitations in S_2). For ideal BCS superconductors,

the cooling power actually diverges logarithmically at $eV = \Delta_1 - \Delta_2$, as was found earlier in Ref. 5. This corresponds to the well known ‘‘ $\Delta_1 - \Delta_2$ singularity matching peak’’ in electric current between two different superconductors at a finite temperature.⁶ In practice, the divergencies are not observed; gap anisotropy and level broadening due to lifetime effects broaden the peaks.

In the experiments, we used aluminum as S_1 and titanium as S_2 . The transition temperatures of our Al and Ti films were $T_{c1} \approx 1.4$ K and $T_{c2} = 0.51$ K, respectively, which are somewhat above the tabulated bulk values. Altogether four samples with slightly different structures were studied, each of which showed cooling of Ti below T_{c2} . In this letter, we concentrate on the experiments performed with the last sample, in which the cooling effect was strongest. A scanning electron microscopy (SEM) micrograph of this sample is presented in Fig. 2, together with a scheme of the electrical connections. The sample was fabricated onto a nitridized silicon substrate using electron beam lithography and three-angle evaporation techniques. Two 15 nm thin aluminum layers were first evaporated at large angles of $\pm 60^\circ$ with respect to the normal of the substrate in the direction of vertical lines of the structure. In this way, the vertical lines were deposited on the substrate, but the narrow horizontal line in the middle was deposited on the walls of the resist in both Al evaporations, and was removed in the liftoff. Aluminum was oxidized in pure O_2 at $p = 10$ mbar for 10 min.

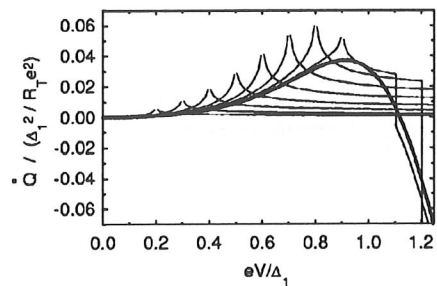


FIG. 1. Calculated heat flow \dot{Q} from S_2 through an ideal S_2/S_1 junction which is biased at voltage V at a constant temperature $T_{e1} = T_{e2} = 0.15\Delta_1/k_B$, which corresponds to 0.37 K for our sample. Different lines have been calculated for $\Delta_2/\Delta_1 = 0$ (NIS structure; thick line), 0.1, 0.2, 0.3, 0.4, 0.5, 0.6, 0.7, and 0.8, respectively. The cooling power diverges when $|eV| = \Delta_1 - \Delta_2$. For our sample, $\Delta_2/\Delta_1 = 0.29$ at $T = 0.37$ K.

^{a)}Electronic mail: antti.manninen@phys.jyu.fi

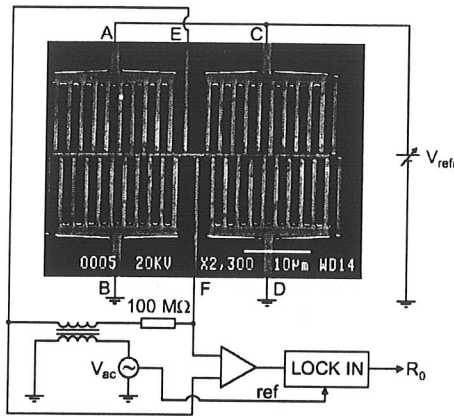


FIG. 2. Scanning electron micrograph of the Al/AIO_x/Ti cooler, and a scheme of the electrical connections. In the SEM micrograph only the titanium parts can be seen; the contrast of the aluminum lines is not good enough for a printed picture. However, each vertical line includes an Al layer which extends across the cooled horizontal Ti line in the middle and makes an Al/AIO_x/Ti tunnel contact with it.

Finally, a 30 nm titanium layer was evaporated directly perpendicular to the substrate. In this way, altogether 42 Al/AIO_x/Ti tunnel junctions were formed between the vertical lines and the 300-nm wide horizontal Ti line in the middle. The 40 junctions which were used for cooling (the comb-like structures A–D in Fig. 2) had an area of about 300×550 nm² and normal-state resistance $R_T \approx 1.9$ kΩ each. The junctions corresponding to E and F, which were used for thermometry, both had an area of about 300×350 nm² and $R_T \approx 3$ kΩ.

We determined the electron temperature of the Ti line, T_{e2} , from the zero-bias resistance, R_0 , of the two Al/AIO_x/Ti tunnel junctions E and F connected in series. The inset of Fig. 3 shows current–voltage (I – V) curves of EF at three different temperatures when Al is superconducting; the I – V curves of the pairs AB and CD were qualitatively similar. When Ti is in normal state, EF forms a SINIS structure and has smooth but strongly temperature-dependent I – V characteristics below the tunneling threshold, $|V| = 2\Delta_1/e \approx 0.42$ meV (where the factor of 2 comes from the two tunnel junctions in series): I decreases and R_0 in-

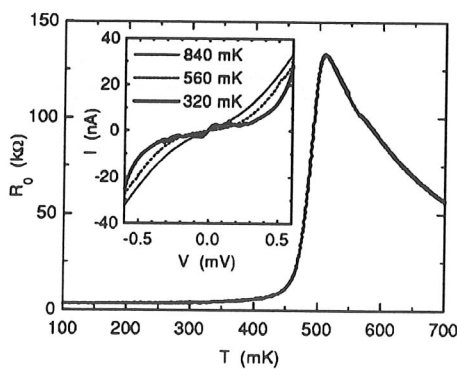


FIG. 3. Temperature dependence of the zero-bias resistance, R_0 , of the Al/AIO_x/Ti junction pair EF of Fig. 2. Titanium becomes superconducting at $T_{c2} = 510$ mK. Inset: current–voltage characteristics of EF at three temperatures.

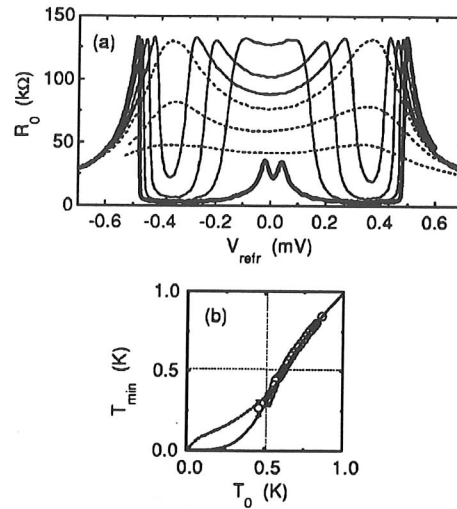


FIG. 4. (a) Zero-bias resistance, R_0 , of the junction pair EF as a function of the voltage, V_{ref} , applied across the “comb-pairs” AB and CD, at different substrate temperatures T_0 . R_0 is related to the temperature of the Ti electrons, T_{e2} , according to Fig. 3. Dashed lines: Ti is in normal state. Thin solid lines: Ti is cooled from normal state to superconducting state. Thick solid line: Ti is superconducting already when $V_{\text{ref}} = 0$. (b) Open circles: measured minimum temperature of Ti, T_{min} , as a function of T_0 . Solid line: T_0 dependence of T_{min} calculated for a SINIS structure. Thick dotted line: T_0 dependence of T_{e2} calculated at $V_{\text{ref}} = 1.9(\Delta_1 - \Delta_2)/e$ for our sample when Ti is superconducting. Thin dotted lines: transition temperature of Ti, $T_{c2} = 0.51$ K.

creases with decreasing temperature. When Ti gets superconducting at $T_{c2} = 510$ mK, a lot of new features develop in the I – V curves at low voltages; this is typical for superconducting double-junction structures with submicron dimensions, in which single charge effects are important.⁷ Some of the features had a hysteretic character, with jumps to different branches in our voltage biased measuring scheme. Most importantly for our thermometry, “supercurrent” appears near zero bias, and R_0 decreases rapidly when temperature decreases below T_{c2} ; note that in submicron junctions the so-called supercurrent is not actual zero-voltage Josephson current but has a maximum at a finite voltage, in the case of Fig. 3 at $|V| \approx 40$ μV. The resistance of the Ti strip itself starts decreasing toward zero at the same temperature; this was checked by a four-wire measurement, feeding current from A to C and measuring voltage across B and D.

The main frame of Fig. 3 shows the temperature dependence of R_0 for EF, when V_{ref} was set to zero (see Fig. 2). The temperature on the horizontal axis was determined by a carbon resistor which was thermally anchored to our sample chamber and calibrated against the primary CBT nanothermometer.⁸ The floating measurement of R_0 was performed by the circuit shown in Fig. 2: using an isolation transformer, a constant alternating current (ac) of about 0.15 nA was fed from E to F, and the voltage across the junctions was measured with a lock-in amplifier.

In Fig. 4 we present the main result of this letter: cooling of Ti to and in the superconducting state by quasiparticle tunneling. The junction pair EF was used for thermometry as explained above. Cooling was achieved by applying a voltage V_{ref} across the “comb-pairs” AB and CD, which were

connected in parallel as shown in Fig. 2. In such a structure, the ohmic losses in the Ti strip due to the cooling current are negligible in spite of the large normal-state resistivity of Ti. When the substrate temperature $T_0 \equiv T(V_{\text{refr}}=0) > 625$ mK, the system is a SINIS cooler and behaves as in the earlier experiments² [see the dashed curves in Fig. 4(a)]; temperature T_{e2} of the electron system of Ti decreases (i.e., R_0 increases) when V_{refr} is applied, reaches a minimum when $|V_{\text{refr}}|$ is slightly below $2\Delta_1/e \approx 0.42$ meV, and starts increasing at higher voltages.

When $T_0 < 625$ mK, R_0 has a deep minimum when V_{refr} is near the value corresponding to the maximum cooling power [see the solid lines in Fig. 4(a)]: Ti cools to superconducting state. For example, when $T_0 = 520$ mK $\approx 1.02T_{c2}$, corresponding to $R_0(V_{\text{refr}}=0) = 127$ k Ω , the minimum temperature reached at $V_{\text{refr}} \approx 0.35$ mV is $T_{\text{min}} \approx (320 \pm 40)$ mK $\approx (0.63 \pm 0.08)T_{c2}$. At substrate temperatures below T_{c2} [thick line in Fig. 4(a)], the Ti strip, interestingly, heats up at very low voltages corresponding to the “supercurrent peak” and then cools down to temperatures below 300 mK; we cannot measure accurately such low temperatures, because R_0 loses its sensitivity to temperature at $T_{e2} \approx 300$ mK (see Fig. 3). The Ti strip is heated up to normal state when $V_{\text{refr}} > 0.5$ mV.

In these experiments only the electrons in Ti cool down, and the lattice temperature T_{p2} stays near T_0 due to the very weak electron-phonon coupling at low temperatures. The minimum temperature, T_{min} , of the Ti electrons is determined by the competition between the cooling power, Eq. (1), and the electron-phonon heat flow,

$$\dot{Q}_{e-p} = \Sigma U(T_{p2}^5 - T_{e2}^5), \quad (2)$$

where U is the volume of the Ti electrode and Σ is a material-dependent constant of order 10^9 W K $^{-5}$ m $^{-3}$. Figure 4(b) shows the measured T_{min} as a function of T_0 . For comparison, we have included the expectations based on Eqs. (1) and (2) both for a SINIS structure and an $S_2IS_1IS_2$ structure with our geometry and materials. In calculations, we used $\Delta_1(0) = 210$ μ eV, $\Delta_2(0) = 77$ μ eV in the $S_2IS_1IS_2$ case, $\Sigma = 1.3 \times 10^9$ W K $^{-5}$ m $^{-3}$ which is of the expected size, and the measured values for R_T and U . We applied the BCS temperature dependence for Δ_1 and Δ_2 , and assumed that $T_{p2} = T_{e1} = T_0$, i.e., that the lattice in Ti and the electrons in Al stay at substrate temperature. In the $S_2IS_1IS_2$ case, we used

\dot{Q} calculated at voltage $V = 0.95(\Delta_1 - \Delta_2)/e$ across each junction as an estimate of the “real” maximum cooling power. The experiments and calculations show that in practice the cooling effect in superconducting Ti is as strong as in a corresponding SINIS structure when $T_{e2} > 0.7T_{c2}$. On the other hand, no clear improvement in the measured cooling power is observed when Ti gets superconducting. When $T_{e2} \ll T_{c2}$, maximal cooling is not observed at $V_{\text{refr}} = 2(\Delta_1 - \Delta_2)/e \approx 0.27$ mV, at which Eq. (1) predicts a diverging \dot{Q} for two junctions in series, but at $V_{\text{refr}} \approx 0.33$ mV. No clear “singularity matching peak” in electric current was observed, either; it was buried under the other features of the I - V characteristics.

In conclusion, we have demonstrated that the electronic cooling method based on tunneling between a superconductor and another metal works even when both metals are superconducting, if the energy gaps are unequal. We have cooled the electron system of a titanium strip with transition temperature $T_{c2} = 0.51$ K from $1.02T_{c2}$ to below $0.7T_{c2}$ by Al/AlO $_x$ /Ti tunneling. This method can be applied for example in bolometric detectors based on the transition edge of superconductivity; their performance improves strongly with decreasing temperature.

The authors thank K. Arutyunov and B. Collaudin for discussions. This work was financially supported by the European Space Agency (ESA), the Technology Development Center of Finland (TEKES), and the Academy of Finland.

¹M. Nahum, T. M. Eiles, and J. M. Martinis, Appl. Phys. Lett. **65**, 3123 (1994).

²M. M. Leivo, J. P. Pekola, and D. V. Averin, Appl. Phys. Lett. **68**, 1996 (1996).

³A. J. Manninen, M. M. Leivo, and J. P. Pekola, Appl. Phys. Lett. **70**, 1885 (1997).

⁴M. M. Leivo, A. J. Manninen, and J. P. Pekola, Appl. Supercond. **5**, 227 (1998).

⁵B. Frank and W. Krech, Phys. Lett. A **235**, 281 (1997).

⁶M. Tinkham, *Introduction to Superconductivity*, 2nd ed. (McCraw-Hill, New York, 1996).

⁷L. J. Geerligs, V. F. Anderegg, J. Romijn, and J. E. Mooij, Phys. Rev. Lett. **65**, 377 (1990).

⁸J. P. Pekola, K. P. Hirvi, J. P. Kauppinen, and M. A. Paalanen, Phys. Rev. Lett. **73**, 2903 (1994); J. P. Kauppinen, K. T. Loberg, A. J. Manninen, J. P. Pekola, and R. A. Voutilainen, Rev. Sci. Instrum. **69**, 4166 (1998).

Trapping of quasiparticles of a nonequilibrium superconductor

J. P. Pekola, D. V. Anghel,^{a)} T. I. Suppala, J. K. Suoknuuti, A. J. Manninen, and M. Manninen

Department of Physics, University of Jyväskylä, P.O. Box 35, 40351 Jyväskylä, Finland

(Received 24 January 2000; accepted for publication 13 March 2000)

We have performed experiments where hot electrons are extracted from a normal metal into a superconductor through a tunnel junction. We have measured the cooling performance of such NIS junctions, especially in the cases where another normal metal electrode, a quasiparticle trap, is attached to the superconductor at different distances from the junction in direct metal-to-metal contact or through an oxide barrier. The direct contact at a submicron distance allows superior thermalization of the superconductor. We have analyzed theoretically the heat transport in this system. From both experiment and theory, it appears that NIS junctions can be used as refrigerators at low temperatures only with quasiparticle traps attached. © 2000 American Institute of Physics. [S0003-6951(00)00219-9]

Selective extraction of electrons from a normal metal conductor (or quasiparticles from a superconductor with a small energy gap) into quasiparticle excitations in a superconductor has recently attracted interest in applying this method in microcooling.¹⁻⁸ Most often a normal metal-insulator-superconductor (NIS) or a symmetric SINIS structure is used to this end. [In what follows we denote NIS or SINIS structures by (SI)NIS wherever the discussion applies to both of them.] Adjusting the voltage across a SINIS structure, one can reduce the temperature of the electrons in the normal metal.

In the first demonstrations of the (SI)NIS coolers^{1,2} the junction areas were very small, typically less than $1 (\mu\text{m})^2$. In the experiments of Ref. 2, a significant reduction of the electronic temperature from 0.3 down to 0.1 K was achieved. In later experiments it has become obvious that a difficult range of operation is at lower bath temperatures, especially below 0.2 K.^{3,9} Here, the geometry of the cooler, the thermalization of the superconductor in particular, is a critical design issue. The cooling power of SINIS structures with such a small junction area is low (typically few pW). Higher cooling power is often needed, and therefore one would wish to employ larger junctions. Yet, if one simply scales up the junction size, the excess quasiparticles in the superconductors have a high probability to return energy back into the normal metal, as discussed theoretically in Ref. 10. In this letter we show experimentally and theoretically how one can remove the excess quasiparticle excitations from the regions near the junctions: we attach a semi-infinite normal metal electrode to the superconductor, forming in this way a bilayer structure, which acts as a "trap" for injected hot quasiparticles.

Experiment: Figure 1(a) shows a test sample where two types of low power SINIS coolers (S =aluminum of 18 nm thickness, I =aluminum oxide, N =copper of 28 nm thickness) can operate on the same normal metal electrode. The

two pairs of junctions, one at the ends of the central normal metal (copper) island (pair A), and another one in the center (pair B), with superconducting electrodes pointing perpendicular to the normal metal island, can alternatively be used, one as a SINIS cooling pair and the other one as a SINIS thermometer. The junctions have different sizes between the pairs $\sim 1 \times 0.3 \mu\text{m}^2$ with total resistance of 12.5 k Ω in A, and $\sim 0.4 \times 0.3 \mu\text{m}^2$ with 34.4 k Ω in B, but more importantly, the superconducting aluminum outside the junctions is covered by a film of copper through the same oxide layer as in the tunnel junctions, differently in the two pairs. In pair B the coverage extends from a distance of about 0.2 μm essentially to infinity, in pair A the similar overlap starts only at a distance of 8 μm . Figure 1(b) shows the corresponding cooling performances. It is obvious that pair B works better as a cooler. This illustrative data show that the cooling characteristics depend on the position of the trap and on the geometry of the junction.

The trap with an oxide layer between the normal metal and the superconductor is not sufficiently effective for large junctions though. To test the efficiency of a normal metal quasiparticle trap, we fabricated different SINIS coolers of nominally $4-6 \mu\text{m} \times 4-6 \mu\text{m}$ overlap area of the NIS junctions. This area is typically two orders of magnitude larger than in the conventional electron beam fabricated junctions.

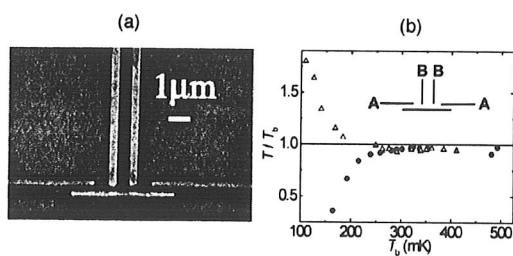


FIG. 1. (a) An SEM image of a basic SINIS cooler with small junctions, schematically shown as an inset in (b). (b) Cooling performance of the sample in (a). Horizontal axis gives the bath temperature. Vertical axis shows the temperature of the normal metal at the optimum cooling bias. The two data sets correspond to: pair B as cooler and pair A as thermometer (circles), and pair A as cooler and pair B as thermometer (triangles).

^{a)}Permanent address: National Institute for Physics and Nuclear Engineering—“Horia Hulubei,” P.O. Box MG-6, R.O.-76900 București-Măgurele, Romania; electronic mail: dragos@phys.jyu.fi

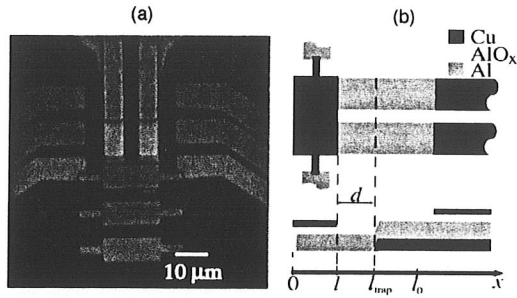


FIG. 2. The SEM image (a) of a large SINIS cooler used in this work, with junction area $\geq 10 \mu\text{m}^2$ and its schematic illustration (b) from above (up) and in cross-section (down). The cooling junction is in the range $[0, l]$, while the bilayer trap starts at the distance l_{trap} from the origin. The parameter l_0 is defined such that $\Delta(x) = \Delta_N$ for $x \geq l_0$. The thick line on top of the Al film [(b) down] represents the oxide layer and forms the junction in the range $[0, l]$.

Figure 2 shows both the schematic drawing and an example of a scanning electron microscope (SEM) image of such a cooler. The coolers were fabricated using silicon nitride mechanical masks.⁹ To allow the fabrication of the quasiparticle traps, three shadows are created. First, a layer of copper (the trap) is deposited at an angle. This is immediately followed by a deposition of aluminum at another angle forming a shadow shifted by a few microns. Aluminum is then oxidized and one more shadow is deposited at a third angle to form the copper island, at a distance d [see Fig. 2 (b)] from the trap. The island overlaps the oxidized aluminum to form the junctions. The sample without the quasiparticle traps is made without the first shadow but otherwise similarly. The small NIS junctions at the ends of the island again serve as thermometers.

Figure 3 shows the maximum temperature drop for five different samples of large SINIS cooler junctions. One cannot compare the performance of different samples quantitatively from the main figure directly, because the junction resistances (R_T) are not equal. Clear qualitative conclusions can, however, be made, especially based on the low temperature behavior. The sample with no quasiparticle trap (filled circles), the one with the trap at a distance $d = 1 \mu\text{m}$, but with an aluminum oxide layer between the two metals forming the bilayer (open down-triangles), and the one with the trap in metal-to-metal contact at $d = 5 \mu\text{m}$ (filled up-triangles) tend to heat up at $T_b \leq 200 \text{ mK}$. The sample shown with open down-triangles had a similar oxide layer between the superconductor and the copper layers to what was used to form the oxide barrier in the (SI)NIS junctions. In the two remaining samples, the one shown with open squares and the one with filled diamonds, the copper-to-aluminum direct metal-to-metal contact is at a distance of less than $1 \mu\text{m}$. One can see that in both cases the cooling performance is superior down to 200 mK and beyond. The difference in performance between these two samples can be explained qualitatively by the difference of R_T in them. (A separate control measurement of a sample with two different values of d from the same fabrication batch were also performed to confirm the conclusion.) The maximum cooling power in the sample shown with open squares, at $T_b = 200 \text{ mK}$, is about 7 pW .

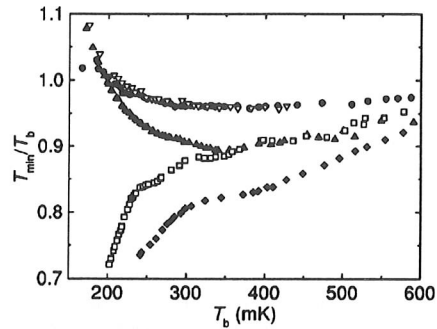


FIG. 3. Performance of large junction SINIS coolers. T_b on the horizontal axis is the starting temperature, and T_{min} is the temperature of the normal electrode at the optimum bias for cooling. The five samples are otherwise similar, but the differing parameters are such that: filled circles—no quasiparticle trap connected, $2R_T = 630 \Omega$; down triangles—quasiparticle trap through an oxide layer at $d = 1 \mu\text{m}$, $2R_T = 280 \Omega$; up triangles—quasiparticle trap in metal-to-metal contact at $d = 5 \mu\text{m}$, $2R_T = 70 \Omega$; open squares—quasiparticle trap in metal-to-metal contact at $d = 1 \mu\text{m}$, $2R_T = 230 \Omega$; filled diamonds—quasiparticle trap in metal-to-metal contact at $d = 1 \mu\text{m}$, $2R_T = 50 \Omega$. The film thickness of the copper trap, aluminum and the normal metal island was 30, 25, and 35 nm, respectively.

Theory: Let us consider the NIS structure presented in Fig. 2(b) (all the geometrical notations will refer to this figure), where the electrons pass from the normal metal into the superconductor. The other junction of the SINIS structure can be treated in a similar manner. By $\Delta(x)$ we denote the nonconstant energy gap of the superconductor. We take the gap energy in a bare Al film to be $\Delta_0 = 200 \mu\text{eV}$, and in the bilayer region $\Delta_N < \Delta_0$ because of the proximity effect, in the case of direct metal-to-metal contact between Cu and Al. The excess quasiparticles in the junction region can disappear or change their energy mainly by one of the following processes: interaction with each other, diffusion, recombination, inelastic scattering on the lattice, and tunneling back into the normal metal. All the last three phenomena heat the normal electrode. To avoid this, we have to decrease the population of the quasiparticle levels by faster diffusion.

Using the energy dependent quasiparticle group velocity, $v(\epsilon, x) = v_F \sqrt{1 - [\Delta(x)/\epsilon]^2}$, where v_F is the Fermi velocity, one can deduce the diffusion constant: $D(\epsilon, x) = [v(\epsilon, x)/v_F] D_n$.¹¹ Here D_n is the diffusion constant of the normal Al film. In the assumption that all the processes are local and if we assign the effective temperatures $T_s(x)$ and T_n to the quasiparticles (in the superconductor) and electrons (in the normal metal), respectively, the diffusion equation of the quasiparticles can be written in the form of a second order differential equation:

$$\begin{aligned} & \left(\frac{d^2 T_s}{dx^2} \right) \int_{\Delta(x)}^{\infty} n_0 D_n \frac{\partial f(\epsilon, T_s)}{\partial T_s} \Big|_x d\epsilon \\ & + \left(\frac{dT_s}{dx} \right)^2 \int_{\Delta(x)}^{\infty} n_0 D_n \frac{\partial^2 f(\epsilon, T_s)}{\partial T_s^2} \Big|_x d\epsilon \\ & - \left(\frac{dT_s}{dx} \right) n_0 D_n \frac{d\Delta(x)}{dx} \frac{\partial f(\Delta, T_s)}{\partial T_s} \Big|_x \\ & - [Y_{\text{rec}}(T_s, x) - Y_{\text{gen}}(T_b, x)] - (Y_{\text{ph}} - Y_{\text{excit}}) \\ & + J_n(U, T_n, T_s(x), x) = 0. \end{aligned} \tag{1}$$

The constant n_0 is the density of electron states at Fermi energy, per unit length, along the x axis, T_b is the bath temperature, and f is the Fermi distribution function. The terms $Y_{\text{rec}}(T_s, x)$, $Y_{\text{gen}} = Y_{\text{rec}}(T_b, x)$, and $(Y_{\text{ph}} - Y_{\text{excit}})$ account for quasiparticle recombination¹¹ and thermal generation rates, and for the inelastic interaction of quasiparticles with phonons, respectively. $J_q[U, T_n, T_s(x), x]$ is the excitation current through the unit length of the junction, at position x .¹⁰ U is the voltage across the junction and $J_q = 0$ for $x > l$. In the case of a trap attached to the superconductor through an oxide barrier, a term corresponding to the tunneling of quasiparticles into the trap is added to the equation above. Eq. (1), together with the heat flow balance equation,¹⁰ gives us all the information regarding the cooling effect. The boundary conditions for Eq. (1) are: $\partial T_s / \partial x = 0$, at $x = 0$ (zero diffusion current), and $T_s = T_b$ at $x \rightarrow \infty$. In the case of a trap in direct metal-to-metal contact we approximate $\Delta(x)$, in the range $0 \leq x \leq l_0$, by the solution of the Ginzburg-Landau equation: $\Delta(x) = -\Delta_0 \tanh\{[x - (l_0 + y_0)] / (\sqrt{2}\xi)\}$. The parameter y_0 is calculated such that $\Delta(x \geq l_0) = \Delta_N$. From the experimental current-voltage curves with different positions of the trap, we could deduce that $1/3 \leq \Delta_N / \Delta_0 \leq 1/2$. D_n , for large junctions, was calculated to be $140 \text{ cm}^2 \text{ s}^{-1}$, from our measured resistivity of the normal Al film, at 4.2 K. Choosing $\xi = 1 \mu\text{m}$ and $l_0 - l_{\text{trap}} = 0.5 \mu\text{m}$ (detailed microscopical calculations should provide better understanding for the density of states) we calculated the minimum temperature of the electron gas in the normal electrode of the large NIS junction, as a function of T_b , taking the extreme values $1/3$ and $1/2$ for Δ_N / Δ_0 , if the trap with metal-to-metal contact was positioned at distances $d = 1, 5,$ and $10 \mu\text{m}$. The results are shown in Fig. 4. Although the cooling performance varies with parameters like the resistance of the junctions (R_T), diffusivity (D_n), and the function $\Delta(x)$, clear conclusions can be drawn: a trap positioned close to the junction vitally improves cooling at low temperature.

Direct numerical calculations and our analytical evaluations show that if there is no trap at all (through the oxide barrier or in metal-to-metal contact), neither small nor large junctions can work as refrigerators at low temperature. The small NIS junctions (as in Fig. 1), with a trap through the oxide barrier positioned close to it, work efficiently as a cooler, while in the case of large NIS junctions, the thermalization of the superconductor is poor at low temperatures, as observed in the experiment.

As a conclusion, we have demonstrated that excess quasiparticle population, i.e., heating up of a superconductor, can be significantly reduced by drawing the hot quasiparti-

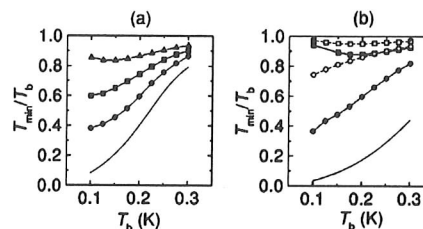


FIG. 4. Theoretical results of the minimum temperature of the normal metal, normalized to the bath temperature, vs bath temperature, for large junctions (the area of one junction is $4 \times 4 \mu\text{m}^2$), in the following situations (see Fig. 3 for corresponding experimental results): (a) $R_T = 110 \Omega$ and $d = 1$ (μm) (circles), 5 (squares), and $10 \mu\text{m}$ (up triangles). $\Delta_N / \Delta_0 = 1/3$; (b) $R_T = 30 \Omega$, $\Delta_N / \Delta_0 = 1/3$, and $d = 1$ (filled circles) and $5 \mu\text{m}$ (filled squares). For comparison we show the corresponding results for $\Delta_N / \Delta_0 = 1/2$, with open circles and squares. The simple solid lines show the cooling results at optimum bias voltage in the ideal cases when $T_s(x) = T_b$ and $\Delta(x) = \Delta_0$ for all x .

cles from the junction region into a bilayer trap. The performance of such a trap is superior even with moderately large power levels, when the trap is in direct metal-to-metal contact at a short ($< 1 \mu\text{m}$) distance from the junction injecting heat (this distance depends mainly on ξ). In smaller junctions, fabricated by regular electron beam lithography, a trap in contact through an oxide barrier seems sufficient for the purpose. We have modeled the heat balance and flow in the (S)NIS—quasiparticle trap systems. The theoretical calculations explain the observed phenomena.

The authors thank the Academy of Finland and European Space Agency for financial support.

- ¹M. Nahum, T. M. Eiles, and J. M. Martinis, Appl. Phys. Lett. **65**, 3123 (1994).
- ²M. M. Leivo, J. P. Pekola, and D. V. Averin, Appl. Phys. Lett. **68**, 1996 (1996).
- ³A. Luukanen, M. M. Leivo, J. K. Suoknuuti, A. J. Manninen, and J. P. Pekola, J. Low Temp. Phys. (to be published).
- ⁴A. J. Manninen, J. K. Suoknuuti, M. M. Leivo, and J. P. Pekola, Appl. Phys. Lett. **74**, 3020 (1999).
- ⁵P. A. Fisher, J. N. Ullom, and M. Nahum, J. Low Temp. Phys. **101**, 561 (1995); Appl. Phys. Lett. **74**, 2705 (1999).
- ⁶D. Chouvaev, L. Kuzmin, M. Tarasov, E. Aderstedt, M. Willander, and T. Claeson, ESA Workshop on Millimetre Wave Technology and Applications, Espoo, Finland, 1998 (unpublished).
- ⁷R. Leoni, G. Arena, M. G. Castellano, and G. Torrioli, J. Appl. Phys. **85**, 3877 (1999).
- ⁸K. Yu. Arutyunov, T. I. Suppala, J. K. Suoknuuti, and J. P. Pekola, J. Appl. Phys. (to be published).
- ⁹J. P. Pekola, A. J. Manninen, M. M. Leivo, K. Yu. Arutyunov, J. K. Suoknuuti, T. I. Suppala, and B. Collaudin, Physica B (to be published).
- ¹⁰J. Jochum, C. Mears, S. Golwala, B. Sadoulet, J. P. Castle, M. F. Cunningham, O. B. Drury, M. Frank, S. E. Labov, F. P. Lipschultz, H. Netel, and B. Neuhauser, J. Appl. Phys. **83**, 3217 (1998).
- ¹¹J. N. Ullom, P. A. Fisher, and M. Nahum, Phys. Rev. B **58**, 8225 (1998).

Efficient Peltier refrigeration by a pair of normal metal/insulator/superconductor junctions

M. M. Leivo and J. P. Pekola

Department of Physics, University of Jyväskylä, P.O. Box 35, 40351 Jyväskylä, Finland

D. V. Averin^{a)}

Department of Physics, SUNY, Stony Brook, New York 11794

(Received 15 September 1995; accepted for publication 31 January 1996)

We suggest and demonstrate in experiment that two normal metal/insulator/superconductor (NIS) tunnel junctions combined in series to form a symmetric SINIS structure can operate as an efficient Peltier refrigerator. Specifically, it is shown that the SINIS structure with normal-state junction resistances 1.0 and 1.1 k Ω is capable of reaching a temperature of about 100 mK starting from 300 mK. We estimate the corresponding cooling power to be 1.5 pW per total junction area of 0.8 μm^2 at $T=300$ mK. © 1996 American Institute of Physics. [S0003-6951(96)02014-5]

Recently it was shown¹ that the Peltier effect in normal metal/insulator/superconductor (NIS) junctions can be used to cool electrons in the normal electrode of the junction below lattice temperature. The cooling arises due to the energy gap in the superconductor, because of which quasiparticles with higher energy are removed more effectively from the normal metal than quasiparticles with lower energy. The decrease in electron temperature demonstrated in this first experiment was, however, limited to about 10% of the starting temperature. There are two possible reasons for this. The first and most obvious, is that the resistance of the refrigerator junction was relatively large leading to low cooling power. The second possible reason is heat leakage through the SN contact used to bias the refrigerator. Nominally, an ideal SN contact with large electron transparency should be able to provide electric conductance without thermal conductance at low temperatures. However both finite temperature and finite subgap density of states in a superconductor lead to nonzero thermal conductance of the biasing contact which degrades the refrigerator performance. This poses the problem of how to bias the refrigerator without compromising its thermal insulation.

In what follows we address these two problems and show that once they are solved the refrigerator performance is improved dramatically. In particular, we show that such a refrigerator is capable of reaching temperatures of about 100 mK starting from 300 mK. This brings the NIS refrigerators quite close to practical applications, for instance, in cooling space-based infrared detectors.²

The problem of refrigerator junction resistance can be alleviated to some degree in a straightforward way either by increasing the junction area or decreasing the specific resistance of the insulator barrier. Because of the limitations of the fabrication method (see below) the junction area could not be increased by much, so that the only option available to us was to make the insulator barrier thinner. Although it is a challenging technological problem to push this process to its limit, we could conveniently reduce the specific resistance of the junctions to about 0.3 k $\Omega \times \mu\text{m}^2$.

It is less obvious how to solve the second problem of

heat leakage through the biasing junction. The solution we suggest here is to combine two NIS junctions in series to form a symmetric SINIS structure. Since the heat current in the NIS junction is a symmetric function of the bias voltage V , the heat flows out of the normal electrode regardless of the direction of the electric current if the junction is biased near the tunneling threshold, $V \approx \pm \Delta/e$. This means that in a symmetric SINIS structure we can realize the conditions when the electric current flows into the normal electrode through one junction and out through the other one, while the heat flows out of the normal electrode through both junctions. In this way the heat leakage into the normal electrode of the structure is minimized. The experiment with the SINIS structures described below supports this idea.

We begin by briefly outlining the basic theoretical concepts concerning the heat flow in the NIS junctions. Under typical conditions when the transparency of the insulator barrier is small, the heat current P out of the normal electrode (cooling power) of an individual NIS junction is:

$$P(V) = \frac{1}{e^2 R_T} \int_{-\infty}^{+\infty} d\epsilon N(\epsilon) (\epsilon - eV) [f_1(\epsilon - eV) - f_2(\epsilon)], \quad (1)$$

where R_T is the normal-state tunneling resistance of the barrier, f_j is an equilibrium distribution of electrons in the j th electrode, and $N(\epsilon) = \Theta(\epsilon^2 - \Delta^2) |\epsilon| / \sqrt{\epsilon^2 - \Delta^2}$ is the density of states in the superconductor. From Eq. (1) we can deduce several properties of the cooling power P . First of all, by changing the integration variable $\epsilon \rightarrow -\epsilon$ we prove that for equal temperatures of the two electrodes P is indeed a symmetric function of the bias voltage, $P(-V) = P(V)$. Plotting Eq. (1) numerically one can see that P is maximum at the optimal bias points $V \approx \pm \Delta/e$. The optimal value of P depends on temperature and is maximum at $k_B T \approx 0.3\Delta$, when it reaches $0.06\Delta^2/e^2 R_T$, and decreases at lower temperatures as $(k_B T/\Delta)^{3/2}$.³ (The last conclusion is different from the T^2 law obtained in Ref. 1.) Specifically, at $V = \Delta/e$ (i.e., quite close to the optimal bias voltage) one can get from Eq. (1):

$$P(\Delta/e) = \frac{\sqrt{\pi}(\sqrt{2}-1)}{4} \zeta\left(\frac{3}{2}\right) \frac{\Delta^2}{e^2 R_T} \left(\frac{k_B T}{\Delta}\right)^{3/2}$$

^{a)}Electronic mail: daverin@ccmail.sunysb.edu

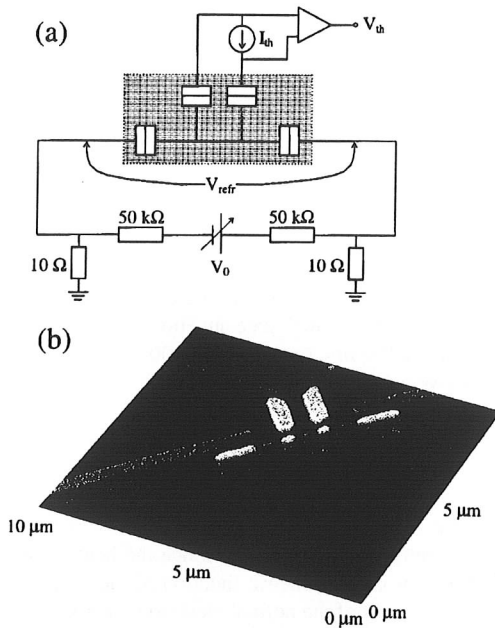


FIG. 1. (a) The schematics of the SINIS refrigerator used in the measurements, and (b) an AFM image of the actual structure.

$$\approx 0.48 \frac{\Delta^2}{e^2 R_T} \left(\frac{k_B T}{\Delta} \right)^{3/2}. \quad (2)$$

Figures 1(a) and 1(b) show, respectively, a schematic diagram of the SINIS structures studied in our experiments and the corresponding antiferromagnetic image of the structure. Four tunnel junctions were fabricated around a normal metal (Cu) central electrode and four superconducting (A1) external electrodes. The electrodes were made with electron beam lithography using the shadow mask evaporation technique. The tunnel junctions were formed by oxidation in pure oxygen between the two metallization steps. Two junctions at the edges with larger areas were used for refrigeration, while the pair of smaller junctions in the middle was used as a thermometer. A floating measurement of voltage across the two thermometer junctions at a constant bias current was used to measure temperature in the same way as in the simpler one junction case.⁴

Prior to our experiments with the SINIS refrigerator we repeated measurements in the geometry of Nahum *et al.*¹ In our case the refrigerating junction had a resistance of $R_T = 7.8 \text{ k}\Omega$, the copper island was $10 \mu\text{m}$ long, $0.3 \mu\text{m}$ wide, and 35 nm thick. Results of the measurements of the electron temperature in the island as a function of refrigerator voltage V_{refr} for several starting temperatures at $V_{refr} = 0$ are shown in Fig. 2. We see that only a few per cent refrigeration can be obtained, as expected.

Solid lines in Fig. 2 represent a theoretical fit obtained within the standard model of electron energy relaxation.⁵⁻⁷ Within this model, we assume that the electron-electron collision rate is large so that the electrons maintain an equilibrium distribution characterized by the temperature T , which is in general different from the lattice temperature T_l . The rate of energy transfer from electrons to phonons is then:⁷

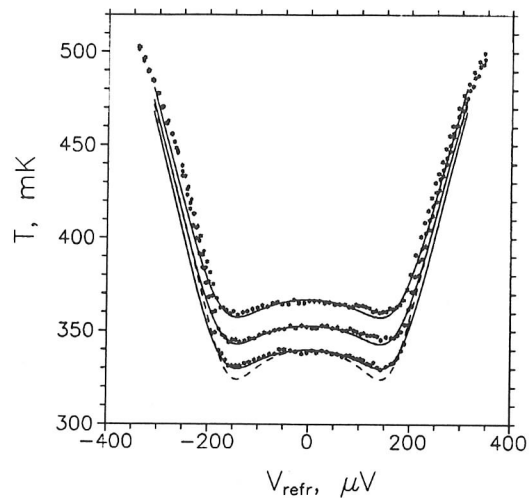


FIG. 2. Results of the NIS single junction experiment: temperature T of the N -electrode vs refrigerator voltage V_{refr} . Dots and solid lines show, respectively, experimental data and the theoretical fit including heat conductance of the biasing contact. For comparison, the dashed line shows the fit without the heat conductance.

$P_l = \Sigma U(T^5 - T_l^5)$, where Σ is a constant which depends on the strength of electron-phonon coupling, and U is the volume of the island. Another element of the fitting process is a heat conductance κ of the biasing SN contact. (For simplicity, we neglect temperature dependence of κ , since the temperature range of interest in Fig. 2 is not very large.) The value of the superconductor gap Δ is almost fixed by the position of the temperature dips in the refrigeration curves (Fig. 2) and is taken to be $155 \mu\text{eV}$ for this sample. Solving numerically the equation $P = P_l + \kappa(T - T_l)$, where P is the cooling power (1) we can calculate T as a function of V_{refr} . The fit in Fig. 2 is obtained in this way with $\Sigma = 0.9 \text{ W/K}^5 \mu\text{m}^3$ and $\kappa = 8 \text{ pW/K}$. For comparison, the dashed line shows the fit obtained for the lowest-temperature curve without κ ; in this case $\Sigma = 1.4 \text{ nW/K}^5 \mu\text{m}^3$. Although there is no drastic disagreement with the data even in this case, we see that κ improves the fit considerably.

To see whether the value of the heat conductance κ deduced from the fit in Fig. 2 is reasonable, we calculated the heat conductance of the SN contact with perfect electron transparency at low temperatures, using the method developed in:^{8,3}

$$\kappa = \frac{2\Delta}{e^2 R_N} \left(\frac{2\pi\Delta}{k_B T} \right)^{1/2} \exp\left(-\frac{\Delta}{k_B T}\right). \quad (3)$$

Making use of the gap value and temperature corresponding to Fig. 2 we get from this equation that $\kappa = 8 \text{ pW/K}$ corresponds to the normal-state contact resistance R_N on the order of 100 Ohm , which is of the same order of magnitude as in the experiment. (It is difficult to obtain a precise value of the contact resistance because it is much less than the resistance of the tunnel junction.)

Figure 3 shows our main results with the SINIS refrigerator of Fig. 1. The two refrigerating junctions had resistances $R_T = 1.0$ and $1.1 \text{ k}\Omega$, respectively, and the island was $5 \mu\text{m}$ long, $0.3 \mu\text{m}$ wide, and 35 nm thick. In Fig. 3 we see

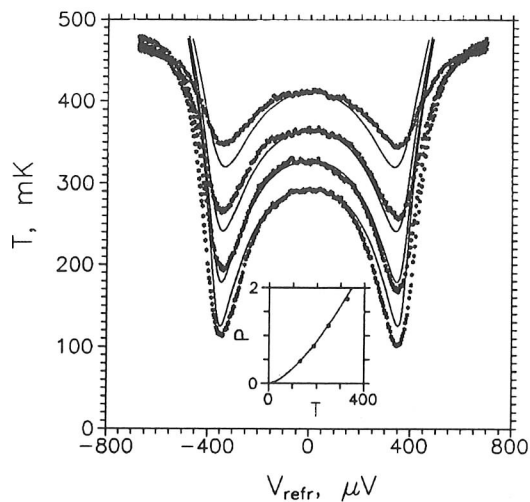


FIG. 3. SINIS refrigerator performance at various starting temperatures. Notations are the same as in Fig. 2. Dots are the experimental data, while the solid lines show the theoretical fit with one fitting parameter Σ for all curves. The inset shows the cooling power P [pW] from the fits (dots), together with the analytical result from Eq. (2).

several refrigeration curves starting at various ambient temperatures at $V_{refr}=0$. Note that maximum cooling power is now obtained at $V_{refr} \approx 2\Delta/e$ because of two junctions involved. From the position of the temperature dips we get $\Delta=180 \mu\text{eV}$. We see that the drop in temperature is immensely improved over that of the single junction configuration. Solid lines in Fig. 3 show the theoretical fit which was obtained within the same model as for the single-junction configuration with the two modifications. We do not have heat conductance κ this time, and we need to solve the balance equations simultaneously for the energy and electric current in order to determine the electric potential of the island. The best fit shown in Fig. 3 corresponds to $\Sigma = 4 \text{ nW/K}^5 \mu\text{m}^3$. The fit can be classified as reasonable, although there are some obvious discrepancies between the data and the theory. Possible origins of these discrepancies include an oversimplified model of electron-phonon heat transfer on the theory side, and poor calibration of the thermometer toward higher temperatures on the experimental side. The inset in Fig. 3 shows the maximum cooling power as a function of temperature deduced from this fit, together with the analytical dependence obtained by summing Eq. (2) over the two junctions. We see that the simple analytical expression (2) gives a very accurate description of the lower-temperature cooling power.

We note in passing that the experiment described above provides a more transparent alternative interpretation of the previous experiments on the enhancement of superconduc-

tivity in the SIS'IS structures.⁹ It implies that the reason for the stimulation of super-conductivity in the central electrode of the SIS'IS structure might not be the formation of the nonequilibrium distribution of quasiparticles inside this electrode,^{9,10} but simply a decrease in its temperature.

Before concluding we would like to mention that the next step in the development of a practical NIS refrigerator could be further optimization of the refrigerator performance with respect to the resistance R_T of the insulator barrier. As we saw above, the cooling power of the refrigerator increases with decreasing R_T . For a fixed junction area this trend would continue only up to an optimal resistance, at which point the transport starts to be dominated by Andreev reflection.³ The theoretical limit for the maximum cooling power density is on the order of $10^{-8} \text{ W}/\mu\text{m}^2$ for aluminum junctions and should be reached in the junctions with unrealistically low specific resistances on the order of $10^{-2} \Omega \times \mu\text{m}^2$. In practice the limiting factors will be the technological ability to fabricate uniform tunnel barriers with high transparency, and, conceivably, the heat leakage through these tunnel barriers to the central island.

In conclusion, we have shown that the nominally symmetric SINIS structure can be used as an efficient Peltier refrigerator. One of the advantages of the symmetric structure is that it is easier to fabricate than the asymmetric single-junction configuration. Besides this, SINIS structure provides more efficient thermal insulation of the central electrode, which allowed us to demonstrate a temperature drop of about 200 mK starting from 300 mK. The achieved cooling power density was approximately $2 \text{ pW}/\mu\text{m}^2$, with the total power being 1.5 pW at $T=300 \text{ mK}$.

The authors gratefully acknowledge useful discussions with K. Likharev and M. Paalanen. This work was supported in part by the Academy of Finland and ONR grant No. N00014-95-1-0762.

¹M. Nahum, T. M. Eiles, and J. M. Martinis, *Appl. Phys. Lett.* **65**, 3123 (1994).

²For space cryogenic applications, see, e.g., C. Hagmann, D. J. Benford, and P. L. Richards, *Cryogenics* **34**, 213 (1994); and a special issue of *Cryogenics* **34**, No. 5 (1994).

³A. Bardas and D. Averin, *Phys. Rev. B* **52**, 12873 (1995).

⁴M. Nahum and J. M. Martinis, *Appl. Phys. Lett.* **63**, 3075 (1993).

⁵M. L. Roukes, M. R. Freeman, R. S. Germain, R. C. Richardson, and M. B. Ketchen, *Phys. Rev. Lett.* **55**, 422 (1985).

⁶F. C. Wellstood, C. Urbina, and J. Clarke, *Appl. Phys. Lett.* **54**, 2599 (1989).

⁷R. L. Kautz, G. Zimmerli, and J. M. Martinis, *J. Appl. Phys. Lett.* **73**, 2386 (1993).

⁸G. E. Blonder, M. Tinkham, and T. M. Klapwijk, *Phys. Rev. B* **25**, 4515 (1982).

⁹M. G. Blamire, E. C. G. Kirk, J. E. Evetts, and T. M. Klapwijk, *Phys. Rev. Lett.* **66**, 220 (1991); D. R. Helsinga and T. M. Klapwijk, *Phys. Rev. B* **47**, 5157 (1993).

¹⁰A. V. Zaitsev, *JETP Lett.* **55**, 66 (1992).

Influence of magnetic field on cooling by normal-insulator–superconductor junctions

K. Yu. Arutyunov,^{a)} T. I. Suppala, J. K. Suoknuuti, and J. P. Pekola
Department of Physics, University of Jyväskylä, PL 35, 40351 Jyväskylä, Finland

(Received 20 December 1999; accepted for publication 29 March 2000)

Cooling by normal-insulator–superconductor junctions in external magnetic field has been studied experimentally. For all orientations of magnetic field the cooling performance correlates with the magnetic field dependent superconducting energy gap $\Delta(H)$. In perpendicular orientation of magnetic field with respect to the sample plane, additional degradation of the cooling power originates from scattering of nonequilibrium quasiparticles in the superconductor on magnetic vortices. The effect is hysteretic and its magnitude depends on the shape of the superconducting probes. © 2000 American Institute of Physics. [S0021-8979(00)02813-9]

I. INTRODUCTION

Normal-insulator–superconductor (NIS) junctions can be used as refrigerators operating at sub-Kelvin temperatures.^{1,2} Biasing a junction at $eV \approx \Delta$, where Δ is the superconductor energy gap, extracts “hot” electrons from the normal N electrode. This results in reduction of electron temperature T_e^N of the N metal. Eventually, at least two mechanisms should be of primary importance for the cooling efficiency of such a device: total heat current extracted by quasiparticles, and the heat exchange between electrons in N metal and the environment. Since SINIS (a symmetric double NIS junction structure) microcoolers are expected to be used in various practical applications, there is a need of their performance optimization under realistic cryogenic conditions, e.g., in a magnetic field. The purpose of the present paper is to study experimentally the influence of external magnetic field on efficiency of electron cooling.

II. EXPERIMENT

The structures were fabricated on nitridized Si substrates using electron beam lithography and three-angle evaporation. A scanning electron microscope image of a typical sample is presented in Fig. 1(a). The central (horizontal) bar is the N electrode (30 nm copper), two pairs of comb-type contacts (A–C and B–G) are superconducting S probes (typically, two aluminum layers \sim 30 nm thick and evaporated at 60°). Insulating barrier was formed by 2 min oxidation of aluminum at 1 mbar pressure of pure oxygen. Additional aluminum contacts (probes E–D) of the same thickness were used as independent electron temperature thermometers. The critical temperature of coevaporated test structures varied from $T = 1.25$ to $T = 1.35$ K depending on aluminum film thickness. A typical measuring procedure consisted of ramping the bias voltage V across the SINIS (A–C, for example) and of simultaneously recording the voltage on the thermometer (another pair: E–D, for example) being current biased close to the gap voltage $V = 2\Delta/e$. The thermometer has been cali-

brated at various magnetic fields against a reference sensor coupled to the cold finger of the dilution refrigerator. Examples of experimental curves illustrating the cooling effect are plotted in Figs. 1(b) and 1(c). Magnetic field was created by a small superconducting solenoid wound around the vacuum jacket of the refrigerator immersed directly into a ⁴He bath. Each experimental curve was obtained in a static magnetic field. Since the characteristic features of interest start to appear at magnetic fields ≥ 5 mT, no special precautions were taken against the ambient magnetic field of the Earth (typically ~ 0.05 mT).

III. BASICS OF NIS COOLER OPERATION

Let us first discuss the influence of magnetic field on the cooling performance due to the change of the total current of the hot electrons extracted from the normal metal N into the superconductor S . Considering the corresponding tunneling probabilities and the Bardeen–Cooper–Schrieffer density of states of a superconductor at low temperatures $T \ll T_c$, the maximum quasiparticle current is achieved at a bias voltage slightly below the energy gap $V \approx \Delta/e$ giving the maximum cooling efficiency of a single NIS junction²

$$\dot{Q}_{\max} \approx 0.6 \frac{\Delta^2}{e^2 R_T} \left(\frac{k_B T_e^N}{\Delta} \right)^{3/2}, \quad (1)$$

where R_T is the tunnel resistance and T_e^N is the electron temperature of the N block. NIS tunneling directly cools the electrons of the normal electrode. Heat exchange with phonons of the N metal will not allow electrons to cool down to infinitely low temperatures. Corresponding electron–phonon heat rate is given as

$$\dot{Q}_{e-ph} = \Sigma \Omega (T_{ph}^{N5} - T_e^{N5}), \quad (2)$$

where Ω is the volume of the N electrode, Σ is a material-dependent constant of order 10^9 W/K⁵ m³, and T_{ph}^N is the phonon (lattice) temperature of the N metal. The phonon system is coupled to the external reservoir (mainly, substrate) of much higher heat capacity and with lattice temperature equal to the bath temperature T_0 . The balance between

^{a)}Author to whom correspondence should be addressed; electronic mail: Konstantin.Arutyunov@phys.jyu.fi

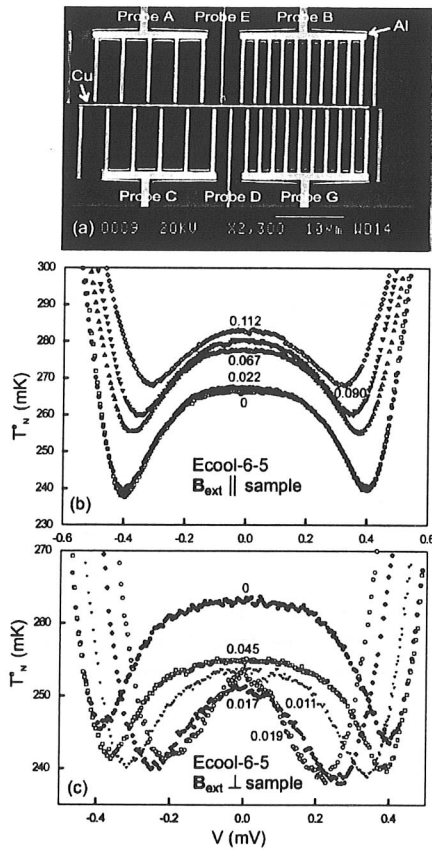


FIG. 1. (a) Scanning electron microscope image of a typical sample. (b), (c) Examples of cooling curves at various magnetic fields: electron temperature T_e^N as a function of the bias voltage V across the SINIS double junction (probes A–C). Numbers close to the curves correspond to external magnetic field B_{ext} measured in teslas. Cooling effect is more strongly suppressed by magnetic field in perpendicular configuration (c) than in parallel orientation (b) with respect to the plane of the structure. Variation of cooling performance at zero magnetic field and slight asymmetry of the curves are due to instability of the bath temperature T_0 . Experiments in parallel (b) and perpendicular (c) orientations were made with 2 days interval when the structure was exposed to atmosphere. Probably, continuous oxidation of the tunnel region caused decrease of the cooling capability, which can be observed as the difference in cooling performance at zero magnetic field in (b) and (c).

cooling power and the electron – phonon exchange rate gives the final steady-state values for the minimum achievable electron temperature T_e^N for given structure parameters and the initial temperature T_0 . Note that the only parameter attributed to the superconductor electrode is the energy gap Δ . This simplified model assumes that there is no backflow of heat from the adjacent S electrode.

IV. EXPERIMENTAL RESULTS AND DISCUSSION

The superconducting gap is suppressed by external magnetic field. Rather straightforward calculations incorporating geometry of the sample and the material-dependent critical field $H_c^{bulk}(0)$ could give the corresponding dependence of the superconducting energy gap on magnetic field and temperature $\Delta(H, T)$. However, in our experiments the energy

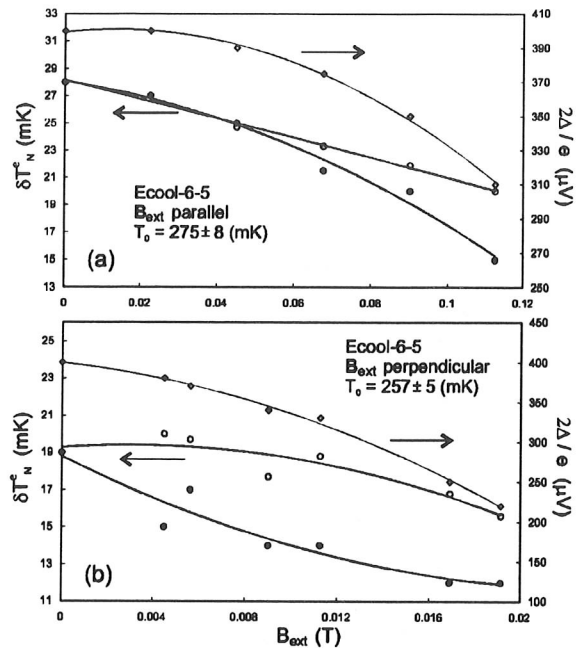


FIG. 2. Dependencies of the maximum change of the electron temperature $\delta T_e^N = T_0 - T_{eMIN}^N$ [left axis, (O) and (●)] and the superconducting energy gap Δ [right axis, (\diamond)] on applied external magnetic field in parallel (a) and perpendicular (b) orientations. For both cases nonmonotonous behavior of $\delta T_e^N(H)$ is due to temporal instability of the bath temperature T_0 . Open circles correspond to calculated values of $\delta T_e^N(H)$ using experimental $\Delta(H)$ data and Eq. (1). Lines are guides to the eye. For perpendicular orientation experimental points (●) are systematically below the calculated values (O).

gap can be directly obtained either from the cooling curves [Figs. 1(b) and 1(c)], corresponding to the bias voltage at which the maximum cooling effect is observed: $eV \approx 2\Delta$, or from current – voltage ($I - V$) characteristics. Figure 2 shows the experimental dependencies of maximum achievable cooling effect $\delta T_e^N = T_0 - T_{eMIN}^N$ and superconducting energy gap Δ on magnetic field H . One can notice that for both parallel and perpendicular orientations of magnetic field there is a correlation between magnetic field dependent energy gap $\Delta(H)$ and the corresponding value of the cooler efficiency $\delta T_e^N(H)$. The reasons for deviations of proportionality at higher fields for perpendicular orientation will be discussed below. Liftoff fabricated superconducting structures fall into the so called “dirty limit”: $\ell \ll \lambda$, ξ , where ℓ is the mean free path, λ is the field penetration depth, and ξ is the superconducting coherence length. Formally, suppression of superconducting energy gap in thin films at small magnetic fields $H < H_{c1}$ (below any vortex structure is allowed) due to pair breaking should be different for parallel and perpendicular orientations.³ However, for both orientations experimentally noticeable degradation of cooling efficiency is observed only at magnetic fields much higher than the first critical field H_{c1} , where additional mechanisms are already efficient. Resuming this part, one can conclude that suppression of the

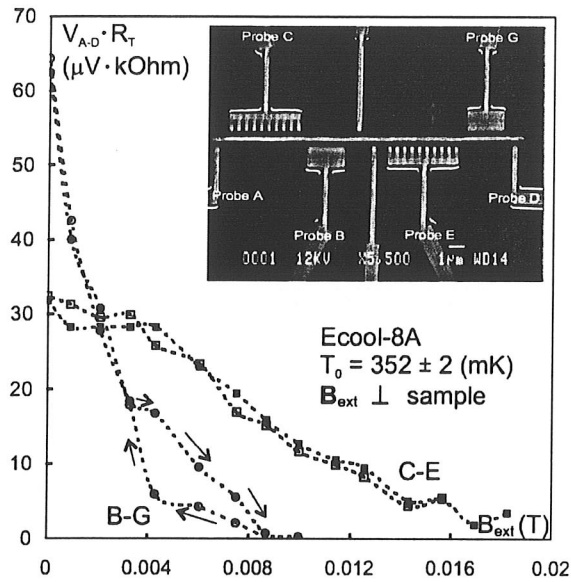


FIG. 3. (Inset) A scanning electron microscope image of the sample with probe notations. Magnetic field dependence of the signal from the “thermometer” V_{A-D} multiplied by the tunnel resistances R_T of the coolers B–G (circles) and C–E (squares), respectively. Filled symbols correspond to successive increase and open ones correspond to decrease of magnetic field. Lines are guides to the eye. V_{A-D} increases when T_c^N drops. Magnetic field is applied perpendicular to the plane of the structure. Areas of the electrodes B–G and C–E are equal. Although “bulk” B–G probes show higher cooling at zero field, their performance is more strongly influenced by magnetic field, than in case of comb-type pair C–E. One can clearly see hysteresis for bulk B–G probes at higher fields.

energy gap by magnetic field qualitatively correlates with the reduction of the cooling performance in accordance with Eq. (1).

If the reduction of the cooling performance of a NIS junction in a magnetic field is only due to a pure pair breaking mechanism [suppression of the energy gap $\Delta(H)$] then, irrespectively of the orientation of the thin film structure in magnetic field, the dependencies of the cooling effect δT_c^N on energy gap $\Delta(H)$ should be the same. However, our experimental observation is different (Fig. 3). In perpendicular orientation the observed dependence of the cooling effect on the energy gap is stronger than the prediction by Eq. (1). This means that there is an additional mechanism of cooling effect suppression by magnetic field in this case.

Conservation of energy requires that the amount of heat removed from the normal part should be dissipated inside the superconductor. But even a much higher power $P_{\text{Joule}} = I \cdot V$ is injected due to the nonzero bias into the superconductor. Heating of the superconductor will result in degradation of the cooling performance.⁴ It is preferable that the extra heat brought to the superconductor by hot quasiparticles is dissipated somewhere far away from the junction region and is absorbed by the thermostat (substrate) of much higher heat capacity than both N and S parts. Heating of the superconductor is governed by the process of nonequilibrium (hot) quasiparticle relaxation. Quasiparticle excitations have finite lifetimes and, hence, being governed by diffusive mo-

tion (in dirty limit) penetrate over a finite length inside a superconductor. It is obvious that to optimize the performance of the NIS cooler it is preferable to make this relaxation length as long as possible. One might expect that magnetic field should reduce the corresponding nonequilibrium lifetimes by at least two ways. First, by introducing an additional scattering mechanism on inhomogeneities of the order parameter created by magnetic field. Second contribution might be expected through alternation of “intrinsic” relaxation mechanisms.

After entering a superconductor nonequilibrium quasiparticles may diffuse into a normal metal in adjacent regions. It has been shown⁴ that forming a normal metal layer on top of the superconductor (without any tunnel barrier) a few microns part from the tunnel region significantly improves cooler operation. Such regions can serve as “quasiparticle traps.” It may turn out that this process is the dominating mechanism of hot quasiparticle relaxation.⁴

Another possibility for quasiparticles to relax is to form Cooper pairs inside the superconductor. In the case of NIS microcoolers nonequilibrium population of quasiparticle excitation spectrum is created via voltage biasing of the tunnel junction. In addition to the recombination process of quasiparticles equally occupying both electron-like and hole-like branches of the excitation spectrum, one should also consider relaxation of inevitably created quasiparticle charge imbalance. Theory of this process has been extensively developed for the case of high temperatures ($T \sim T_c$).⁵ Unfortunately, the opposite case of low temperatures has not been well addressed. However, as optimal bias voltages of the cooler are close to the energy gap $eV_{\text{bias}}^{\text{cooler}} \approx eV_{\text{gap}}^{\text{cooler}} = \Delta$, one may assume that charge imbalance is not significant. Hereafter we consider recombination of quasiparticles as if the number of hole-like and electron-like excitations would be equal.

Relaxation of nonequilibrium quasiparticles with energies $E \sim \Delta$ to condensate at Fermi level should be mediated by a nonelastic process. At low temperatures possible “microscopic” mechanisms of relaxation are: electron – phonon scattering, electron–electron interaction and scattering on magnetic impurities. In the case of aluminum, magnetic impurities might be excluded.

Phonon-mediated recombination time τ_R can be calculated as follows:⁶

$$\frac{1}{\tau_R} = \frac{\sqrt{\pi}}{\tau_0} \left(\frac{2\Delta}{k_B T_c} \right)^{5/2} \left(\frac{T}{T_c} \right)^{1/2} e^{-\Delta/k_B T_c}, \quad (3)$$

where τ_0 is a material dependent parameter of the order of effective electron – phonon relaxation time. It depends on temperature and the purity of the sample. For aluminum thin film structures $\tau_0 \sim 100$ ns.^{6,7} One can estimate the corresponding length over which the excitations will penetrate into a superconductor before recombining into Cooper pairs: $\Lambda_Q = \sqrt{D\tau_R}$, where the diffusion coefficient $D = \frac{1}{3}v_F\ell$ and the Fermi velocity for aluminum is $v_F(\text{Al}) = 1.3 \times 10^6$ m/s. Contrary to Refs. 7 and 8 we neglect the deviation of the quasiparticle diffusivity from the corresponding value in normal state. Substituting typical values ($\ell = 30$ nm, $T_c = 1.3$ K) into Eq. (3) and temperatures suitable for NIS cooler (~ 200 mK) one gets $\Lambda_Q^{\text{ph}} \geq 1$ mm. At the same moment, it

was obtained experimentally, that positioning a normal metal on top of the *S* electrode (quasiparticle trap) at a distance larger than a few microns from the NIS junction changes nothing, while if the corresponding distance is about 1 μm it improves the cooler operation. One may conclude that phonon-mediated recombination is not the dominating process. Regular diffusion of the quasiparticles is responsible for the observed effects.⁴

Electron – electron interaction at low temperatures and corresponding dephasing times is a “hot” topic widely discussed now.^{9,10} How electron – electron interaction contributes to relaxation of nonequilibrium quasiparticles in a superconductor at temperatures much below its energy gap $T \sim 200 \text{ mK} \ll T_c \sim 1.3 \text{ K}$ is not clear. However, it seems that at low temperatures and at zero magnetic field there are no other mechanisms which could account for inelastic relaxation processes of sufficient intensity except electron – electron scattering.

Certainly, if the details of the main mechanism of relaxation are not clear, there is not much hope for estimating magnetic field corrections. The only prediction we could probably make is that application of magnetic field will not increase the corresponding relaxation time (length). However, as will be shown below, at magnetic fields where degradation of cooling performance becomes noticeable, one should consider another effective mechanism of relaxation: scattering of quasiparticles on magnetic vortices.

Type-I superconductors in a form of a thin film behave like type-II superconductors if the thickness $d < \sqrt{5}\lambda$, where $\lambda = \lambda(T)$ is the temperature dependent field penetration depth.³ At magnetic fields higher than the first critical field $H_{c1}(T)$ external field penetrates into a superconductor in the form of flux vortices. This threshold field is given by

$$H_{c1}(T) = (1 - \eta)H_c^{\text{bulk}}(T) \frac{\ln \kappa}{\kappa \sqrt{2}}, \quad (4)$$

where $H_c^{\text{bulk}}(0)$ is the thermodynamic critical field ($\approx 10 \text{ mT}$ for aluminum), η is the demagnetization factor, and $\kappa = \lambda/\xi$ is the Ginzburg – Landau parameter, which for dirty limit materials is reduced to $\kappa = \lambda_L/\ell$, λ_L being the London penetration depth in pure material.³ The mean free path ℓ can be obtained experimentally from the sample resistance at liquid helium temperature (4.2 K) since $\rho/\ell \approx 4 \times 10^{-16} \Omega \text{ m}^2$ for aluminum. Approximating the shape of the superconducting probes [“comb fingers”, Fig. 1(a)] by an ellipsoid, one can estimate the corresponding demagnetization factors. Substitution of the sample parameters into Eq. (4) gives the values for the $H_{c1}^{\perp}(0)$ as small as $\sim 0.1 \text{ mT}$ for perpendicular orientation. Above this value the sample should be in a mixed state characterized by the presence of an Abrikosov vortex lattice.

Each vortex has a characteristic size of the quasnormal core region of the order of superconducting coherence length $\xi(T)$. The corresponding cross section of quasiparticle scattering on a vortex might be of the same order.⁷ In the case of our thin film structures in the dirty limit, $\xi(0) = 0.85(\xi_n/\ell)^{1/2} \approx 180 \text{ nm}$, which is larger than the film thickness ($\sim 30 \text{ nm}$). So, there is no room for vortices in parallel

orientation of the film. Vortex penetration for parallel magnetic fields should be significantly suspended in comparison with the case of perpendicular orientation. In reality, the plane of a sample is always tilted with respect to magnetic field and finally vortices do penetrate. But this effect is much smaller than in the case of perpendicular configuration. This difference experimentally manifests itself in the following way: the cooling effect in parallel orientation is still noticeable up to $\sim 0.1 \text{ T}$, while in the perpendicular case no cooling is observed at fields higher than $\sim 20 \text{ mT}$ [Figs. 1(b) and 1(c), respectively]. It should be noted that in our experiments alignment of the sample with respect to magnetic field was done with an accuracy of $\Delta\varphi = \pm 5^\circ$. Better alignment in parallel configuration should result in further increase of the cooling performance in the high field limit.

To enter (or exit) a superconductor each vortex should overcome a potential barrier at sample imperfections (including the surface). In practice, vortices start to penetrate into a superconductor at fields higher than the corresponding first critical field H_{c1} and go away at lower fields being pinned to imperfections. Thus, penetration of vortices is a hysteretic process. As has been already discussed, the magnitude of cooling in NIS junctions should depend on heating of the superconducting electrode, which is related to relaxation of nonequilibrium quasiparticles. Certainly, the relaxation process is dependent on mechanisms of quasiparticle scattering. Consequently, one might expect the corresponding hysteresis of cooling efficiency at sufficiently high magnetic fields. Figure 3 illustrates the above statement. In perpendicular orientation cooling efficiency gradually reduces with the increase of magnetic field due to the corresponding increase of the density of vortices, which act as quasiparticle scatterers. After surpassing a certain value of irreversibility H^{irr} , the original cooling dependencies do not repeat on decreasing the applied field. Vortices are pinned to sample imperfections and as the temperature is low $T \sim 200 \text{ mK} \ll T_c \sim 1.3 \text{ K}$, thermal activation of the vortex jumps is inefficient. One should reduce significantly the external magnetic field to let vortices reconfigure into the initial “equilibrium” distribution. Observation of the hysteresis in the cooling effect strongly supports our assumption that the formation of an Abrikosov vortex lattice manifests itself as an additional mechanism of scattering of nonequilibrium quasiparticles. Note that in large samples (large area, large perimeter) irreversibility threshold H^{irr} should correlate with corresponding first critical field H_{c1} exceeding this value only due to the potential barrier at the edges. In mesoscopic-size superconducting objects in small fields the actual density of vortices $\sigma_\phi^{\text{actual}}$ might be significantly smaller than the corresponding equilibrium value $\sigma_\phi^{\text{eq}} = B/\phi_0$. In this case the irreversibility field should rather correspond to formation of the first vortex: $H^{\text{irr}} \sim \phi_0/A_s^{\text{eff}}$, where A_s^{eff} is the *S* probe area. Experimental values of irreversibility threshold fields H^{irr} are about $\sim 5 \text{ mT}$ (Fig. 3) giving the effective area $A_s^{\text{eff}} \sim 0.5 \mu\text{m}^2$. The effective area of superconducting probe A_s^{eff} corresponds only to the adjacent junction *S* region where quasiparticle relaxation takes place and not to the whole area of the aluminum pad. In the rest part of the superconducting electrode covered with normal metal (quasiparticle trap) recombina-

tion of hot quasiparticles into equilibrium charge carriers is the dominant mechanism of relaxation.

Note that no corresponding hysteresis has been detected in parallel orientation at fields up to ~ 0.1 T, when the superconducting gap has already been strongly suppressed and the cooling effect was very small. In quasiparallel orientations density of magnetic vortices is too small to make the corresponding scattering mechanism competitive. For this configuration the observed degradation of the cooling effect at high magnetic fields should be attributed either to suppression of the energy gap $\Delta(H)$, or to other nonvortex-related mechanisms of quasiparticle scattering.

V. OPTIMIZATION OF NIS COOLER SHAPE

Operation of NIS coolers in magnetic field is an important issue in practical applications. There is a need for elaboration of the device design with maximum immunity against external magnetic field. In perpendicular orientation of the structure plane with respect to magnetic field the cooling effect is suppressed more strongly than in the parallel case. Hereafter we will mainly discuss the former configuration, keeping in mind that in all practical realizations finite normal component of magnetic field is always present due to inevitable misalignment.

To increase the cooling power [Eq. (1)] the total quasiparticle current should be increased, which requires reduction of the tunnel resistance R_T . Decrease of the tunnel resistance by thinner insulating layers has definite technological limits. Such tunnel barriers are not very reliable due to high probability of pinhole formation, shorting the N and S electrodes. An alternative solution is to increase the total area of NIS junctions.

Still there is a freedom in selecting the shape of the superconducting electrode to optimize the operation. To solve this question a microcooler containing three pairs of SINIS junctions was fabricated (Fig. 3). As usual, one pair (A–D) served as an electron temperature sensor. Pairs B–G and E–C had the same total area of the tunnel junction and of superconducting electrode, but pair B–G had a conventional rectangular form ($2 \mu\text{m} \times 2 \mu\text{m}$), while pair E–C was formed from ten “fingers” each $0.2 \mu\text{m} \times 2 \mu\text{m}$. Corresponding cooling dependencies in the perpendicular field are presented in Fig. 3. One should note that although the “rectangular” cooler has higher cooling effect at zero magnetic field, its performance is more strongly suppressed by magnetic field, than in case of comb-type probes. In our structures the effective diameter of the magnetic flux core is about ~ 180 nm. The width of each comb finger is of the same order (~ 200 nm). There is not enough room for vortices to fit into such a narrow bar. In the case of “bulk” electrode, sample geometry allows vortices to enter the probe, acting like quasiparticle scatterers contributing to stronger suppression of the cooling performance by magnetic field. Even in the larger “rectangular” probes the total number of vortices at the highest fields (~ 15 mT) is $N_\phi^{\text{eq}} = \Phi / \phi_0 \sim 15$, where

Φ is the total magnetic flux threading the superconducting probe: $\Phi = B \cdot A_s^{\text{eff}}$. In equilibrium in comb-like probes with the same overall area there should be an equal number of vortices. However, to enter a superconductor each vortex has to overcome a potential barrier at the sample boundary. For the same total area, a sample with larger boundary (perimeter) is supposed to have smaller density of vortices: $\sigma_\phi^{\text{actual}} < B / \phi_0$. The smaller the sample (fewer vortices) the more important the last nonequality. Thus, small area S probes with large perimeter are of advantage against the magnetic field.

Further decrease of the S probe linewidth much below the size of a vortex core (\sim superconducting coherence length ξ) is unreasonable. First, NIS junctions formed of very narrow lines are subject to continuous barrier degradation due to oxidation “from sides.” Second, reduction of the linewidth (typically, only few times larger than the film thickness) causes decrease of the mean free path ℓ . This effect inevitably manifests itself in the reduction of quasiparticle relaxation time (length) leading to more intensive heating of the S electrode in proximity to the junction region. Eventually, the poorer cooling performance at zero magnetic field of the comb-type cooler in comparison with the “rectangular” one (Fig. 3) is due to these effects.

Our NIS microcoolers appear to be much less sensitive to magnetic field (in perpendicular orientation) than the corresponding devices used in Refs. 7 and 8. This is probably a result of much smaller areas of superconducting probes used in our experiments. In Ref. 7 it was found that the existence of vortex lattice at fields as small as ~ 0.2 mT already caused noticeable losses.

ACKNOWLEDGMENTS

The authors would like to acknowledge J. M. Ullom for valuable discussions, the European Space Agency (Contract No. 13006/98/NL/PA(SC)), and the Russian Foundation for Basic Research (Grant No. 98-02-16850) for financial support.

- ¹M. Nahum, T. M. Eiles, and J. M. Martinis, *Appl. Phys. Lett.* **65**, 3123 (1994).
- ²M. M. Leivo, J. P. Pekola, and D. V. Averin, *Appl. Phys. Lett.* **68**, 1996 (1996).
- ³M. Tinkham, *Introduction to Superconductivity*, 2nd ed. (McGraw-Hill, New York, 1996).
- ⁴J. P. Pekola, D. V. Anghel, T. I. Suppala, J. K. Suoknuuti, A. J. Manninen, and M. Manninen, *Appl. Phys. Lett.* (to be published).
- ⁵J. Clark, in *Nonequilibrium Superconductivity, Phonons and Kapitza Boundaries*, edited by K. E. Gray (Plenum, New York, 1981).
- ⁶S. B. Kaplan, C. C. Chi, D. N. Langenberg, J. J. Chang, S. Jafarey, and D. J. Scalapino, *Phys. Rev. B* **14**, 4854 (1976).
- ⁷J. N. Ullom, PhD dissertation, Harvard University, Cambridge, 1999.
- ⁸J. N. Ullom, P. A. Fisher, and M. Nahum, *Appl. Phys. Lett.* **73**, 2494 (1998).
- ⁹B. Altshuler, XXII International Conference on Low Temperature Physics, Abstracts, Helsinki, August 4–11, 1999, p. 391.
- ¹⁰D. S. Golubev and A. D. Zaikin, XXII International Conference on Low Temperature Physics, Abstracts, Helsinki, August 4–11, 1999, p. 391.